7-11-2022

Numerical Modeling of Pile Responses under Lateral Loading Considering the Scour Effects

Jungmin Lee
Louisiana State University and Agricultural and Mechanical College

NUMERICAL MODELING OF PILE RESPONSES UNDER LATERAL LOADING CONSIDERING THE SCOUR EFFECTS

A Thesis

Submitted to the Graduate Faculty of the
Louisiana State University and
Agricultural and Mechanical College
in partial fulfillment of the
requirements for the degree of
Master of Science in Civil Engineering

in

The Department of Civil and Environmental Engineering

by
Jungmin Lee
B.S., Seoul National University of Science and Technology, 2011
M.E., Seoul National University of Science and Technology, 2013
August 2022

ACKNOWLEDGEMENTS

I would like to express my thanks to the committee chair, Dr. Shengli Chen, and other committees, Dr. Murad Abu-Farsakh and Dr. Hai Lin to complete this thesis.

Especially, I would express my thanks and gratitude to my advisor, Dr. Shengli Chen. He has supported me a lot to finish this thesis. He gave me important comments, suggestions, knowledge, etc. to understand the basic theory and improve the problem-solving skill, not only geotechnical field also other related science and engineering field. Further, his critical questions, approach, and guideline to solve geotechnical problems make me be able to see a specific geotechnical problem in a variety of views, so finally my boundary of geotechnical knowledge would be expanded. Moreover, because of his clear advice and instruction, I can focus on finishing my thesis in the right direction/way.

Special thanks are going to go to Edris Akbari for the numerical modeling. The finite element software which I used for this thesis was quite new for me, so I am sure that I could not understand details about the software without his comments. I can make my thesis more solid based on his suggestions and insights about the numerical analysis and FE software.

Additionally, I want to say thank the research lab members, Chang Huang and Xu Wang, for their open-mind, encouragement, kindness, etc. Last, I always appreciate my family members' unconditional love and encouragement.

TABLE OF CONTENTS

LIST OF TABLES

LIST OF FIGURES

ABSTRACT

This thesis focuses on the 3D numerical analysis of the laterally loaded pile. For numerical modeling/analysis, ABAQUS, a widely used commercial software, is used. Non-scour and scour conditions are considered for this thesis. Two elastoplastic constitutive models, Mohr-Coulomb model and Cam Clay model, are applied. Unknown material and interface properties are calibrated based on two references which explained the numerical analysis of the laterally loaded pile under the non-scour condition. Different cases of scour depth, S_d, scour width, S_w, and scour slope angle, α, are applied for the laterally loaded pile analysis under the scour condition.

From the results of the numerical analysis under the scour condition, scour depth, S_d, can be the main factor for the pile capacity changes. Scour width, S_w, and scour slope angle, α, are also the other factors which have an influence on the reaction force changes of the laterally loaded pile. This thesis also describes the plastic deformation/strain results of the laterally loaded pile analysis. From the plastic strain results depending on the scour width, the plastic strain appears on the scour slope when the scour width is narrow. On the other hand, when scour width is sufficiently wide, the plastic strain distribution would be similar to the one when the scour width is infinite. This strain distribution state can be shown in both Mohr-Coulomb model and Cam Clay model. In the view of the scour slope angle, the plastic strain in Cam Clay model is more smoothly expanded onto the scour slope than Mohr-Coulomb model.

CHAPTER 1. INTRODUCTION

1.1 Overview

Scour is the soil loss due to erosion in river bottoms or in waterfront areas (Coduto, 2001). One of the possibilities that scour can be generated is the fact that soil around and beneath foundations can be washed away due to the fluid flow. For a laterally loaded pile foundation, the pile usually resists the lateral load by passive earth pressure in its surrounding soil, so scour is one of the critical reasons for the stability of the laterally loaded pile. Based on this reason, scour is one of the important factors to design shallow and deep foundations of bridge, piers, wind turbine, and other structures. The AASHTO LRFD Bridge Design Specification (2010) mentions that scour is the major reason for bridge failure in the United State (Chavan et al, 2022).

Many researches of the pile scour have been progressed by both experimental tests and numerical analysis. For example, in particular the numerical analysis of pile scour, scour can be modeled by reducing apparent fixity length, setting the stiffness corresponding to p-y and t-z curve of Winkler models, or modeling the geometry by FE analysis (Jia, 2018). However, most researches focus on pile deflection and p-y curves under the lateral loading, and it is seldom easy to find researches which focus on soil, for example, soil deformation, especially plastic deformation/strain, stress and pore water pressure distribution, etc. Further, although scour geometry is also one of the pivotal factors for pile scour analysis, the scour geometry is less considered.

Therefore, this study would discuss the numerical analysis of pile response under lateral loading considering scour effect. Furthermore, numerical analysis would show lateral load-pile

deflection curves and the plastic strain distribution of soil depending on scour width, depth, and slope slope.

1.2 Research Objective

This thesis describes pile response under lateral loading considering scour effect using finite element method. For the finite element method, ABAQUS would be used to this study.

The objective of this thesis is as below:

a) Establish finite element modeling for the laterally loaded pile without scour effect. Two elastoplastic constitutive models would be applied: Mohr Coulomb model and Cam Clay model.

b) Calibrate material and interface properties for pile deflection numerical modeling. Finite element analysis results will be compared to the field data results.

c) Establish finite element modeling for the laterally loaded pile with scour condition based on the finite element analysis without scour condition. Scour depth, width, and scour slope angle are considered in this finite element analysis. Furthermore, describe the laterally loaded pile behavior and plastic deformation/strain of soil.

1.3 Research Procedure

This study has two main steps: numerical modeling of pile deflection without and with scour conditions. The numerical analysis without scour condition would be performed first. In this step, material and interface properties can be calibrated based on two field test data. After the

numerical modeling without consideration of the scour condition/effect, the numerical analysis under scour condition would then be carried out. Parametric study would then be performed. Details of this study would be followed as below (see **Figure 1**),

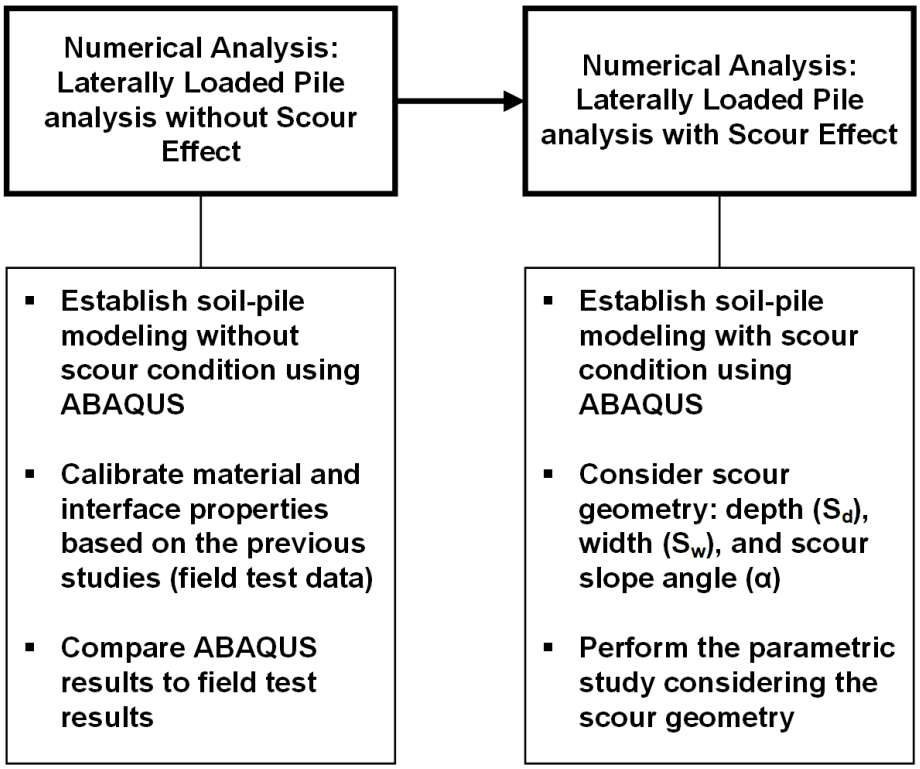

Figure 1. Details of this study

1.4 Thesis Outline

This thesis has 5 chapters as below,

a) CHAPTER 1 is introduction to explain the brief overview, study objective, and research procedure.

b) CHAPTER 2 presents the literature review about a laterally loaded pile in soft clay and numerical analysis of pile scour.

c) CHAPTER 3 describes laterally loaded pile analysis without scour effect. This chapter shows the procedure of FE analysis. Calibration of material and interface properties is also conducted. Results of FE analysis are shown pertaining to two elastoplastic constitutive models, i.e., Mohr-Coulomb model and Cam-Clay model.

d) CHAPTER 4 presents laterally loaded pile analysis with scour effect. Parametric study is carried out, and the three main parameters which are related to the scour geometry are applied. The calibrated material and interface properties in CHAPTER 3 are used. Pile response under the lateral loading and plastic deformation/strain distribution would be presented.

e) CHAPTER 5 ends with the conclusions obtained/summarized from this thesis. Recommendations for further study are given.

CHAPTER 2. LITERATURE REVIEW

2.1 Introduction

The objective of this thesis is the investigation of a laterally loaded pile response in clay under the scour effect by numerical analysis. This chapter would describe the literature review about the laterally loaded pile in soft clay and numerical analysis of the laterally loaded pile analysis under the scour effect.

2.2 Laterally Loaded Pile in Soft Clay

2.2.1 Matlock (1970)

Matlock (1970) suggested the *p-y* curve for static loading in soft clay based on the field test of a laterally loaded pile at Lake Austin, Texas. The formula proposed by Matlock (1970) is as below (see **Eq. (1)**),

$$\frac{p}{p_u} = 0.5\left(\frac{y}{y_c}\right)^{\frac{1}{3}} \tag{1}$$

where, p = lateral soil resistance, p_u = the ultimate resistance of pile, y = pile deflection, y_c = The pile deflection at 50 % of maximum stress

In soft clay, the ultimate resistance of a pile, p_u, can be expressed as **Eq. (2)**,

$$p_u = N_p c d \tag{2}$$

where, c = the soil strength, d = the pile diameter, and N_p = a nondimensional ultimate resistance coefficient

Matlock also suggests two formulae of N_p (**Eq. (3) and (4)**), and the smaller value of N_p would be used.

$$N_p = \left(3 + \frac{\sigma_x}{c} + J\frac{x}{d}\right) \tag{3}$$

$$N_p = 9 \tag{4}$$

where, σ_x = overburden pressure from the soil itself, J = coefficient (approximately 0.5 based on studies of Sabine data), x = depth

The pile deflection at 50 % of maximum stress, y_c, can be calculated using Skepmtom's approach (see **Eq. (5)**),

$$y_c = 2.5\varepsilon_c d \tag{5}$$

where, ε_c = the strain at 50 % of maximum stress (the range of ε_c is between 0.005 and 0.02, 0.01 for most purpose)

2.2.2 Lin et al. (2014)

Lin et al. (2014) focus on two key parameters, the effective unit weight, γ', and the undrained shear strength, C_u, to establish the modified *p-y* curve. In scour condition, the effective unit weight, γ', would be changed depending on void ratio and overburden stress. Further, the changes of the undrained shear strength can be presented by Critical State Soil Mechanics, and the changes would be expressed by overconsolidation ratio, OCR.

The modified formulae of the ultimate resistance of a pile, p_u, considering the effective unit weight, γ', and the undrained shear strength, C_u, are as below (Lin et al, 2014),

$$p_{ult1} = (OCR)^{\Lambda}\gamma'_{sc}z(3D + Jz)\left[\frac{(C_u)_{int}}{(z + S_d)\gamma'_{int}}\right] + \gamma'_{sc}zD \tag{6}$$

$$p_{ult2} = 9D(OCR)^{\Lambda}\gamma'_{sc}z\left[\frac{(C_u)_{int}}{(z+S_d)\gamma'_{int}}\right] \tag{7}$$

where, γ'_{int} = soil effective unit weight before scour, γ'_{sc} = soil effective unit weight after scour, $(C_u)_{int}$ = undrained shear strength before scour, z = soil depth measured from the ground surface, D = the pile width, Λ = approximately 0.8, J = coefficient, S_d = the scour depth

Overconsolidation ratio, OCR, can be obtained using **Eq. (8)**,

$$OCR = \frac{\gamma'_{int}(S_d + z)}{\gamma'_{sc}z} \tag{8}$$

2.2.3 Zhang et al. (2017)

Zhang et al. (2017) also propose two equations of the ultimate resistance of a pile, p_u, considering both the effect of scour hole dimensions and stress history. The proposed formulae are as below,

$$\begin{aligned} p_{ult1} = [3D + J(z - S_d)]C_u^{int}&\left(\frac{(3-2\sin\varphi')OCR}{1+2(1-\sin\varphi')OCR^{\sin\varphi'}}\right)^{\Lambda-1} \\ &+\left\{\nu_{int}\gamma'/\left[\nu_{int} + \kappa\ln\left(\frac{(3-2\sin\varphi')OCR}{1+2(1-\sin\varphi')OCR^{\sin\varphi'}}\right)\right]\right\}(z-S_d)D \end{aligned} \tag{9}$$

$$p_{ult2} = 9\mathrm{D}C_u^{int}\left(\frac{(3-2\sin\varphi')OCR}{1+2(1-\sin\varphi')OCR^{\sin\varphi'}}\right)^{\Lambda-1} \tag{10}$$

where, γ' = soil effective unit weight, ν_{int} = the specific volume before scour, φ' = soil internal friction angle, C_u^{int} = undrained shear strength before scour, κ = the swelling index, z = soil depth measured from the ground surface, D = the pile width, Λ = approximately 0.8, J = coefficient, S_d = the scour depth

2.3 Numerical Analysis of Pile Scour

Many researches of pile scour have been progressed: both experimental and numerical research. According to Richardson et al. (2001) and Briaud et al. (1999), pile scour significantly depends on the shear stress by fluid flow that the fluid flows tangentially to soil surface at soil-water interface. Further, the shear stress, especially critical shear stress, τ_c, is also imposed by water when pile scour is initiated. The method of SRICOS which means Scour Rate In Cohesive Soils is applied to measure scour depth in cohesive soil, i.e. clay. Based on Briaud's previous research, Briaud (2015) and his team develop a measurement method of pile scour based on large-scale laboratory tests. To measure the scour depth of piles in clay and sand soil, flow and soil properties, in particular the critical velocity or critical shear stress, are important.

Chen et al. (1993) perform a numerical analysis that combines the infinite and finite element method to better-understand pile-soil interaction under later loading using AVPULL program. In this research, ungrained shear strength, c_u, and normal and shear stiffness of interface parameters between a pile and its surrounding soil are key parameters to measure the ultimate soil resistance. Lin et al. (2019), Dao (2011), and Kim et al. (2011) choose PLAXIS, one of the world-widely used finite element analysis software, to analyze lateral pile behavior. Lin et al. (2019) analyze the lateral pile behavior in sand soil. The factors, which affect the lateral pile behavior, are scour depth, scour width, scour slope, and pile dimension. The interesting thing is that Kim et al. (2011) mention there is no significant influence between the interface properties and the modulus of subgrade reaction. Li et al. (2013) choose FLAC3D to compare numerical results with field data and perform the parametric study. In Li's research, Mohr-Coulomb model is applied.

For interface properties, Kim et al. (2011) choose R_{inter}, interface strength reduction factor, which PLAXIS provides. In this paper, non-associated flow rule and Mohr-Coulomb model are

adopted for soil layers, so the bilinear Mohr-Coulomb model is employed for pile-soil interface element properties. Yang et al. (2002) show one thin layer of element for an interface layer between a pile and its surrounding soil, and Drucker-Prager model is applied to simulate and control interface element properties, tangential and normal stiffness of the interface element. The widely used commercial software, ABAQUS can also provide an interface model, and Mardfekri et al. (2013) study nonlinear soil-pile interactions for laterally loaded single piles. In Mardfekri's paper, pile scour is not considered, but deformed mesh (soil deformation) depending on pile deflection and soil-pile interface is shown. Further, Mohr-Coulomb model is applied for soil-pile interface properties.

He et al. (2019) present the investigation of the stress history effect with a monopile supported offshore wind turbine under scour condition in soft clay using a three-dimensional finite element method. ABAQUS, the world-widely used numerical analysis software, is adopted. For soil condition, an advanced hypoplastic clay model is applied for soil stiffness and strength on stress history. Further, the interface behavior between the monopile and its surrounding soil is simulated under the Coulomb friction law. Wang et al. (2020) also show ABAQUS scour effect modeling with the Mises yield criterion and isotropic hardening model. However, a drawback of He et al. (2019) and Wang et al. (2020) are that the whole scour layer is removed (S_w = infinite), and this is significantly different comparing with Zhang et al. (2017), Liang et al. (2018), and Lin et al. (2016) that the scour hole is considered. Guo et al. (2022) also carry out 3D finite element analysis using ABAQUS considering the scour depth and the angle of the scour hole.

Ashour et al. (1998) choose strain-wedge model to measure soil resistance with free-headed pile in normally consolidated clay, and effective unit weight, plasticity index, effective friction angle, the strain of 50 % maximum stress, and undrained shear strength are key parameters in this

paper. Skempton's equation is applied to obtain the effective stress with excess pore water pressure. Moreover, the strain wedge model depends on the modulus of subgrade reaction, E_s, which shows the soil-pile interaction at any level during pile loading or soil strain. Lin et al (2016) show two wedge models: wedge failure model considering scour hole and equivalent wedge failure model without scour hole to measure soil resistance. The paper published by Zhang et al. (2021) show the closed-form analytical solution using by Boussinesq's point load solution, and this analytical solution can obtain the reduced effective stress at any point depending on scour unloading.

Among Liang et al. (2018), Zhang et al. (2017) and Lin et al. (2014) choose the p-y curve, which is purposed by Matlock (1970) and critical state soil mechanics for stress history in clay. Still, effective unit weight, the strain of 50 % maximum stress, and undrained shear strength are key parameters. The significant difference between Zhang et al. (2017) and Lin et al. (2014) is whether the scour-hole geometry/dimension is applied to analyze a laterally loaded pile. For sand, Yang et al. (2010) show that state-dependent shear strength, and effective friction angle can be calculated by the theory of critical soil mechanics.

Most of the research show results of bending moment, pile deflection, and p-y curve along the pile axis. Lin et al. (2020) show soil stress distribution depending on the laterally loaded pile. In Lin's work, stress distribution analysis of pile groups is carried out using by Mohr-Coulomb model for the soil properties.

2.4 Summary

Based on previous studies, most studies focus on the bending moment of the pile, pile deflection with respect to the depth, and p-y curve depending on pile scour width, depth, and slope;

however, the stress distribution study related to pile scour width, depth, and slope, pile type has not been done yet. Further, Mohr-Coulomb model for soil properties is the main constitutive model to investigate stress distribution, and especially there is the limited study of stress distribution depending on stress history using by Cam-Clay model.

CHAPTER 3. LATERALLY LOADED PILE MODELING WITHOUT SCOUR CONDITION

3.1 Introduction

CHAPTER 3 would describe the preliminary numerical analysis of a laterally loaded pile and its results about 3-dimensional finite element analysis without scour condition. For numerical modeling, it uses ABAQUS, which is a widely-used commercial software, to analyze the laterally loaded pile. The numerical analysis would be carried out with two elastoplastic constitutive models: Mohr-Coulomb model and Cam-Clay model. A closed-ended steel pipe pile is adopted. There is difficulty to put the lateral load on the center of the pile head due to the geometry of a pipe pile, so a reference point with the rigid body constraint on the center of the pile head is used. DCM (displacement control method) is applied to control the lateral load on the pile head. Scour condition is not considered in this chapter. Results of numerical analysis are shown as pile responses under the lateral load.

3.2 Laterally Loaded Pile Modeling without Scour Condition using ABAQUS

3.2.1 Step, Load, and Boundary module

There are three steps of laterally loaded pile modeling using ABAQUS: initial, geostatic, and loading steps (see **Figure 2**). The initial step includes setting up initial geostatic stress, pore water pressure, and void ratio. Boundary condition controlled by Displacement/Rotation would be set up in the initial step. A roller type of boundary condition is placed in x and y directions, and a fixed type of boundary condition is arranged in z direction. Ground water boundary by Pore Pressure in Boundary Condition is also placed on the ground surface.

The second step is geostatic to verify initial stress equilibrium with pore water pressure. The keyword *GEOSTATIC which ABAQUS provides is applied to check the initial stress equilibrium in the geostatic step. Geostatic Stress in Predefined Field is adopted to set up initial vertical and horizontal stresses with the lateral earth pressure coefficient, K_0, value depending on the soil depth, z. In this case, the initial vertical and horizontal stresses are linearly distributed. Pore water pressure can be defined by Pore Pressure in Predefined Field.

The third step is loading steps using keyword *Static, General in Mohr-Coulomb model and *Soil, Consolidation in Cam-Clay model. Lateral load is applied in the loading steps, and the total number of loading steps is 11 steps with respect to time, t. For the lateral load, DCM (Displacement Control Method) is applied with the fact that loading speed is equal to 0.0005 m/s, instead of LCM (Load Control Method).

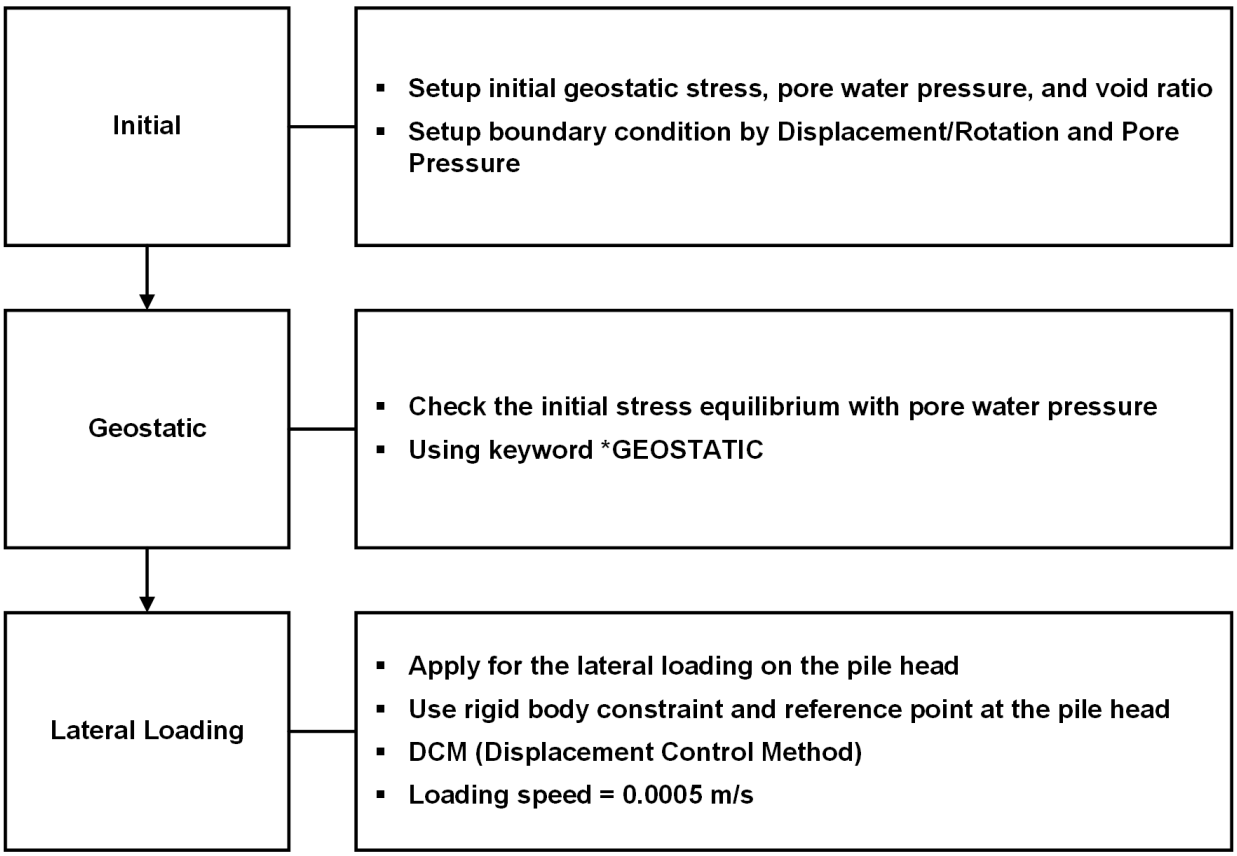

Figure 2. The procedure of the laterally loaded pile FE analysis without the scour condition

3.2.2 Interface Elements and Properties for the Laterally Loaded Pile

One of the pivotal factors for the pile analysis is interface elements and interface properties (see **Figure 3**). Interface element and properties allow the sliding motion between a pile and its surrounding soil. This sliding behavior due to the interface elements and properties affect the vertically loaded pile analysis results. Lee et al. (2014) perform 2D pile numerical analysis under a vertical load, and this research shows the vertical load-pile displacement curve depending on interface properties. Various vertical load-pile displacement curves are shown depending on interface properties, and it means that both interface elements and properties are one of the important factors for establishing the sliding behavior between a pile and its surrounding soil of the vertical loaded pile analysis.

However, in the case of the laterally loaded pile analysis, it seems that the interface properties of the laterally loaded pile analysis might have less influence on pile responses under a lateral load compared with the vertically loaded pile analysis; nevertheless, the interface elements and properties are still required because the sliding movement between a pile and soil still appears in the front side of the pile along the lateral load. In addition, Potts et al. (2001) show the lateral load-displacement curve for the undrained lateral loading of a single pile with and without interface elements. The lateral load-displacement curve shows a large gap between the laterally loaded pile analysis with and without interface elements. This gap can occur because interface elements cannot sustain the tensile normal stresses, so the interface elements allow opening between a pile and its surrounding soil when the interface elements have experienced the tensile normal stresses. Then, this opening is called “gapping” as shown in **Figure 4 (a)**. **Figure 4 (b)** shows ABAQUS U, Magnitude result reproduced based on Li et al. (2013). Both sliding and gapping behavior are visible in **Figure 4 (b)**.

ABAQUS provides zero-thickness interface elements and interface properties to model the friction behavior between a pile and its surrounding soil based on Coulomb friction law. In this study, penalty method (friction coefficient) in tangential behavior and "Hard" contact in normal behavior are used. "Hard" contact in normal behavior can allow surface separation between pile and soil when the contact pressure reaches to zero. Additionally, for interaction behavior, a master surface on a pile and a slave surface on soil are selected based on the ABAQUS manual guideline (see **Figure 5**), which mentions the surface on the stiffer body should act as the master surface. Therefore, the pile surface would be master surface, and the slave surface would be placed in the soil surface.

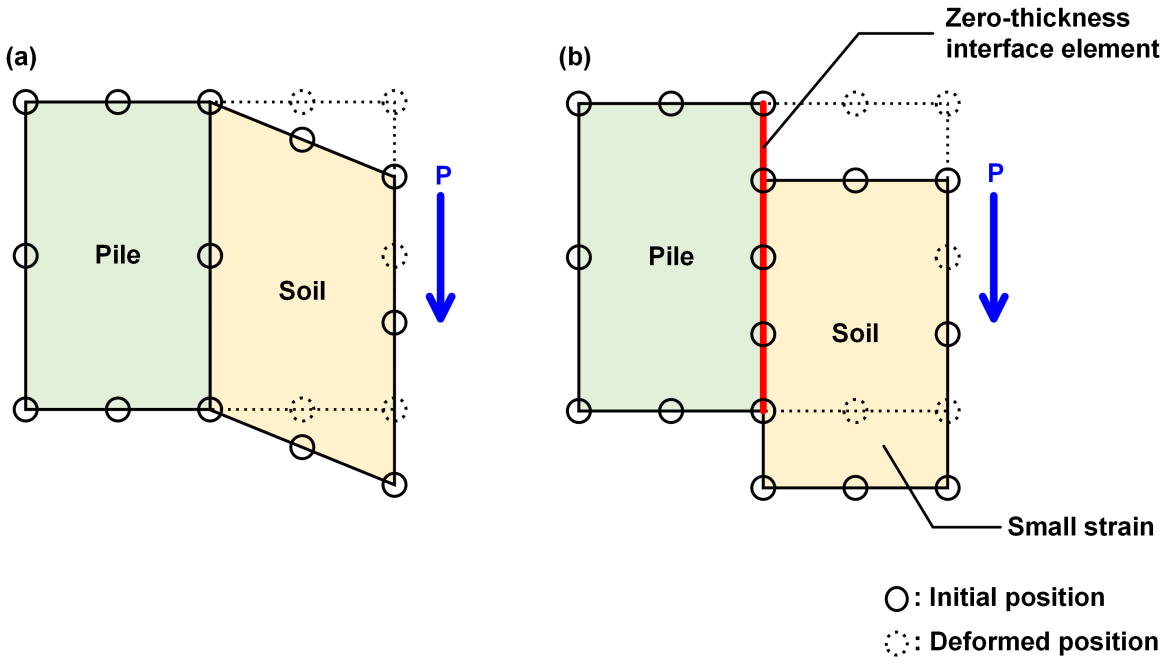

Figure 3. Interface element for the vertically loaded pile: (a) no interface element, (b) zero-thickness interface element between pile and soil (Potts et al, 1999)

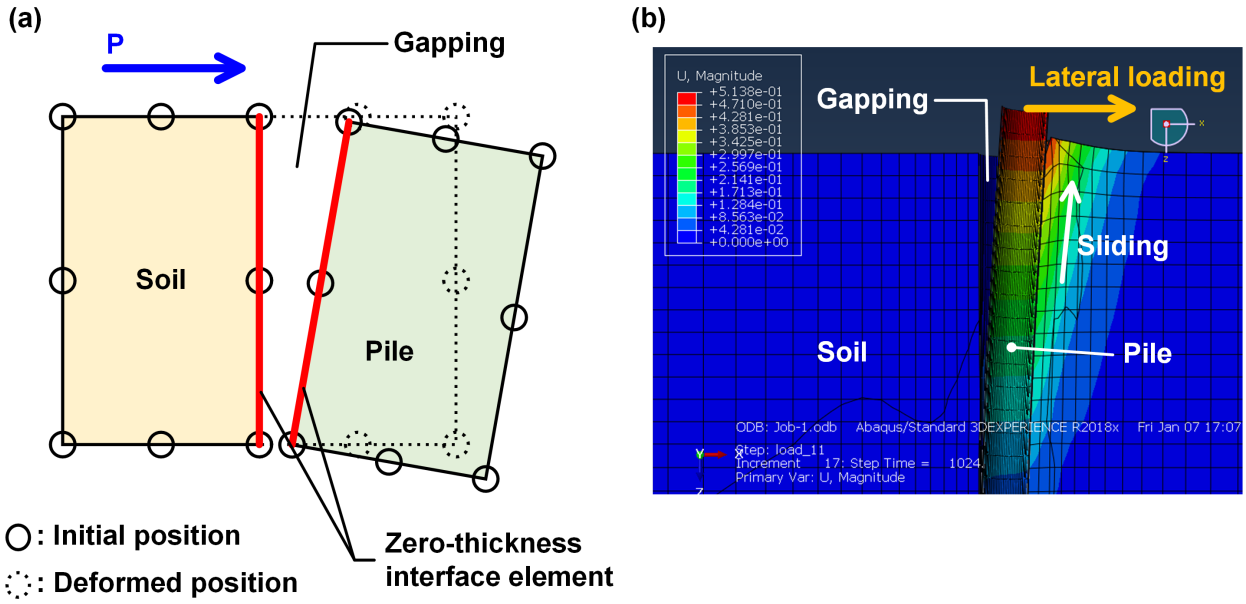

Figure 4. Interface element for the laterally loaded pile: (a) gapping between soil and a pile, (b) gapping in ABAQUS results (Li et al. 2013)

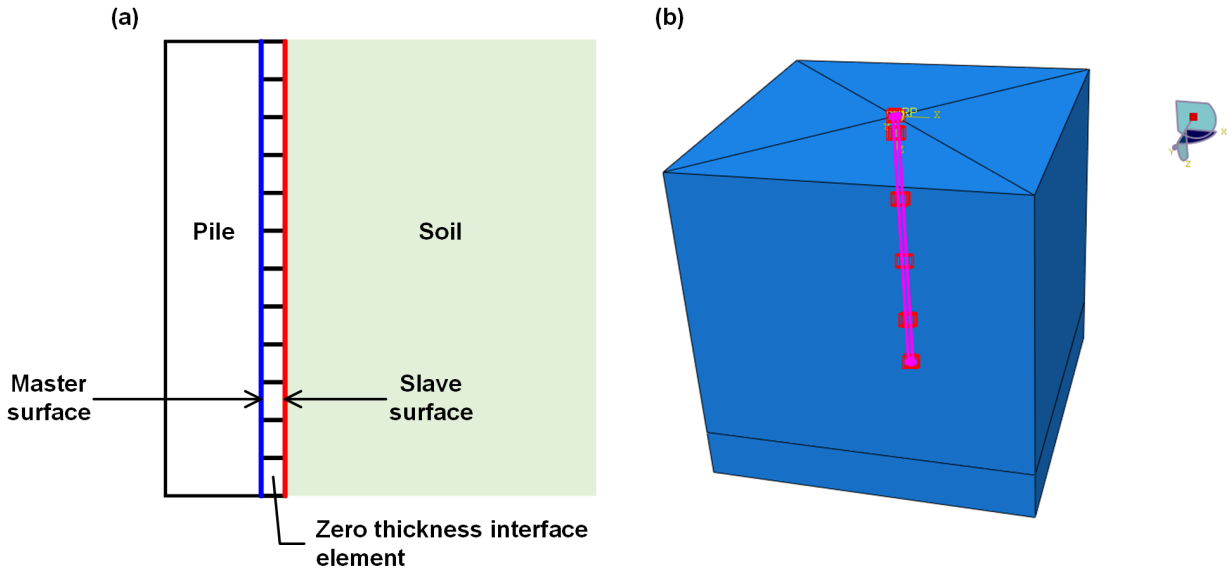

Figure 5. Interface elements between a pile and soil: (a) the location of master and slave surfaces, (b) master and slave surfaces in ABAQUS

3.3 Numerical Modeling with Mohr-Coulomb Model

The laterally loaded pile analysis with Mohr-Coulomb model is performed based on Kim et al. (2011) and Li et al. (2013). Both Kim et al. (2011) and Li et al. (2013) perform the finite element analysis of the laterally loaded pile based on the field test at Incheon grand bridge construction site, South Korea. For the laterally loaded pile finite element analysis, Kim et al. (2011) choose *PLAXIS 3D* Foundation, and Li et al. (2013) use *FLAC 3D* version 4.0.

3.3.1 Geometry and Mesh of Pile Deflection Analysis

As shown in **Figure 6**, there are 5 soil layers in the ground: upper marine clay, lower marine clay, silt, residual soil, and weathered rock. Each soil layer has different depth. The total boundary of soil is dimensioned by the width of 40 m and the depth of 27.4 m size. The pile is modeled by the closed-ended steel pipe pile with the diameter of 1.016 m, the thickness of 16 mm, the embedded length of 25.6 m, and the eccentricity of 1 m. The lateral load would be applied to the reference point on the pile head.

Stress near the pile would be changed drastically when the lateral load is applied on the pile head, so, for mesh, small mesh can be arranged to determine the exact result of stress changes. For this reason, single-bias seeds are applied to arrange each seed and control the distance between a seed and a seed. Short seed distance near the pile would be arranged, and this short seed distance can create small mesh. Based on the seed distance, small meshes are placed near the pile The element type is C3D8 (An 8-noded linear brick) for both soil and pile mesh (see **Figure 7**).

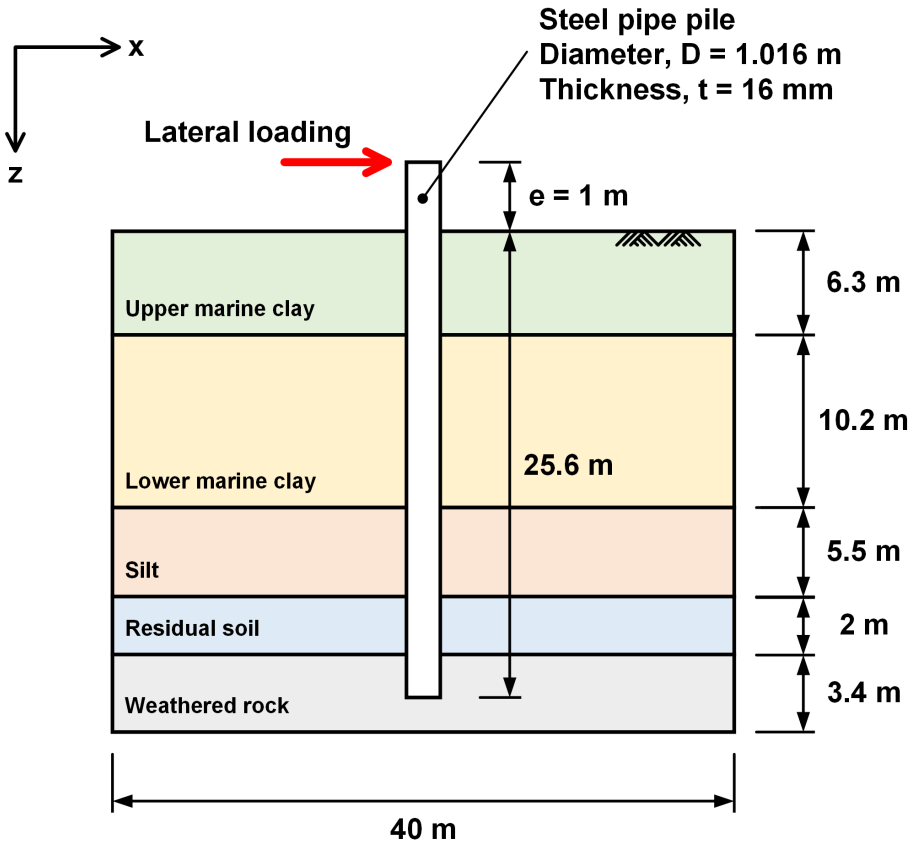

Figure 6. Geometry for FE analysis with Mohr-Coulomb model (Li et al, 2013)

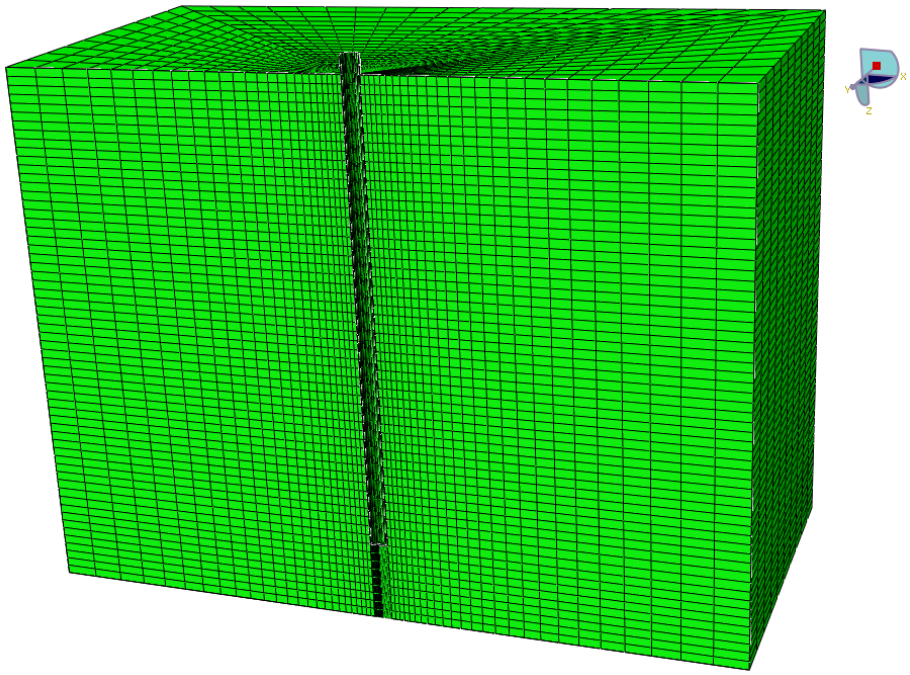

Figure 7. Laterally loaded pile modeling with Mohr-Coulomb model by ABAQUS

3.3.2 Material and Interface Properties

Mohr-Coulomb model is applied for upper and lower clay, silt, and residual soil, and weathered rock and a pile are modeled by Linear-Elastic model. Material and interface properties are summarized in **Table 1** and **Table 2**. Material properties by Kim et al. (2013) are adopted. Clay usually can be explained by cohesion, c, and friction angle, ϕ, is the main parameter for sand, so friction angle, ϕ, for clay and cohesion, c, for sand can assume zero. Linear-elastic model does not need cohesion, c, and friction angle, ϕ. For interface properties (see **Table 2**), Kim et al (2011) choose several interface properties for each soil layer, but Li et al (2013) choose single interface properties. In this study, the single tangential behavior is used, and the value of tangential behavior, μ, is equal to 0.8.

Table 1. Material properties for FE analysis with Mohr-Coulomb model (Kim et al. 2011)

Layer	**Model**	**Density, ρ (kg/m^3)**	**Young's Modulus, E (MPa)**	**Poisson's Ratio, ν**	**Cohesion, c (kPa)**	**Friction Angle, ϕ (°)**
Upper Clay	M-C	1750	10	0.3	18	0
Lower Clay	M-C	1750	23	0.3	42	0
Silt	M-C	1780	27	0.3	70	0
Residual Soil	M-C	1780	35	0.3	0	34
Weathered Rock	L-E	2020	11	0.25	-	-
Pile	L-E	7200	200,000	0.2	-	-

*M-C is Mohr Coulomb model, and L-E is Linear Elastic model.

Table 2. Interface properties for FE analysis with Mohr-Coulomb model (Li et al. 2013)

Interface Properties	
Tangential Behavior	0.8
Normal Behavior	"Hard" Contact

3.3.3 Results of FE Analysis

Figure 8 shows the lateral load vs. pile deflection curve comparing ABAQUS results to Li's numerical analysis results based on the calibrated material and interface properties. ABAQUS result shows good agreement with Li et al. (2013), and this means that the material and interface properties are calibrated and verified. These calibrated material and interface properties would be used to the numerical analysis of the laterally loaded pile under scour condition in the CHAPTER 4.

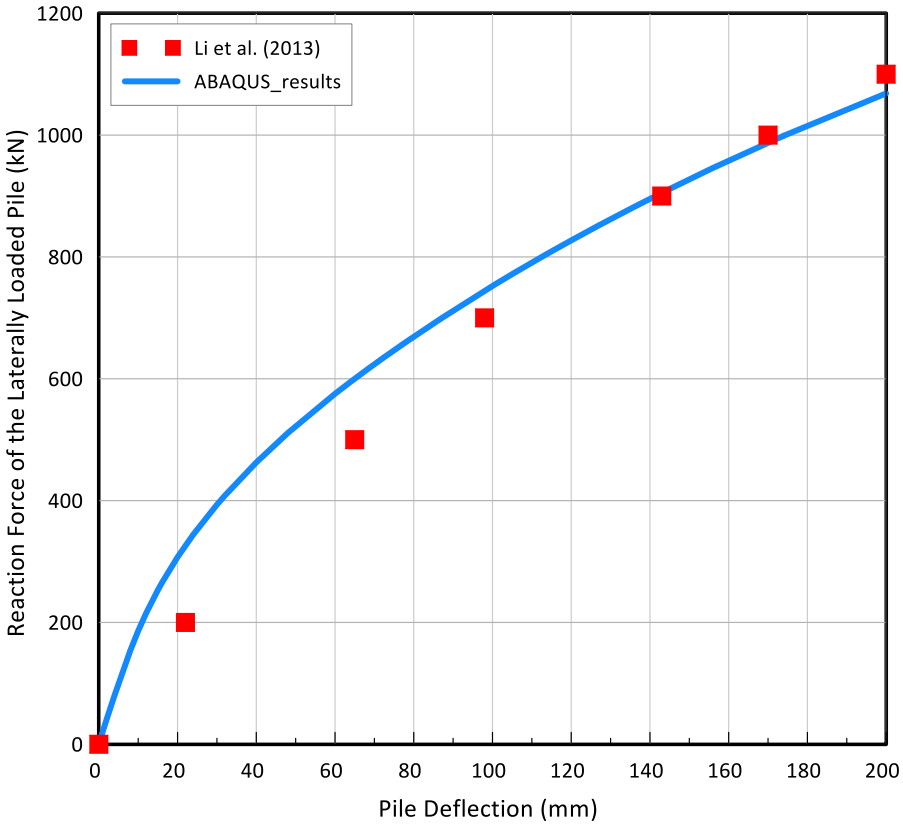

Figure 8. Lateral Load vs. Pile deflection curve compared ABAQUS results to Li et al. (2013)

3.4 Numerical Modeling with Cam-Clay Model

Laterally loaded pile analysis with Cam-Clay model is performed based on Lin et al. (2014 and 2016) using Matlock (1970)'s field test data. Matlock (1970) shows the results based on the field test data at Lake Austin, Texas, and Lin et al. (2014) perform the finite element analysis of the laterally loaded pile based on Matlock's field test results using by the commercial software *LPILE 5.0*. In Lin et al. (2016), *FLAC 3D* is used to analyze the laterally loaded pile response. This numerical modeling with Cam-Clay model is performed based on Lin's finite element analysis.

3.4.1 Geometry of Pile Deflection Analysis

As shown in **Figure 9**, there is a single layer in soft clay. The boundary of soil is dimensioned by the width of 15 m and the depth of 15 m size. The pile is modeled by the closed-ended steel pipe pile with the diameter of 0.319 m, the thickness of 0.0127 mm, the total pile length of 12.8 m, and the eccentricity of 0.06 m. The lateral load would be applied to the reference point at the pile head.

In the same manner as the previous pile analysis with Mohr-Coulomb model, short seed distance near the pile would be arranged, and small meshes are generated near the pile. The element type for soil is C3D8P (An 8-node brick, trilinear displacement, trilinear pore pressure), and the pile element type is C3D8 (An 8-noded linear brick). ABAQUS modeling of Cam-Clay model is shown as **Figure 10**.

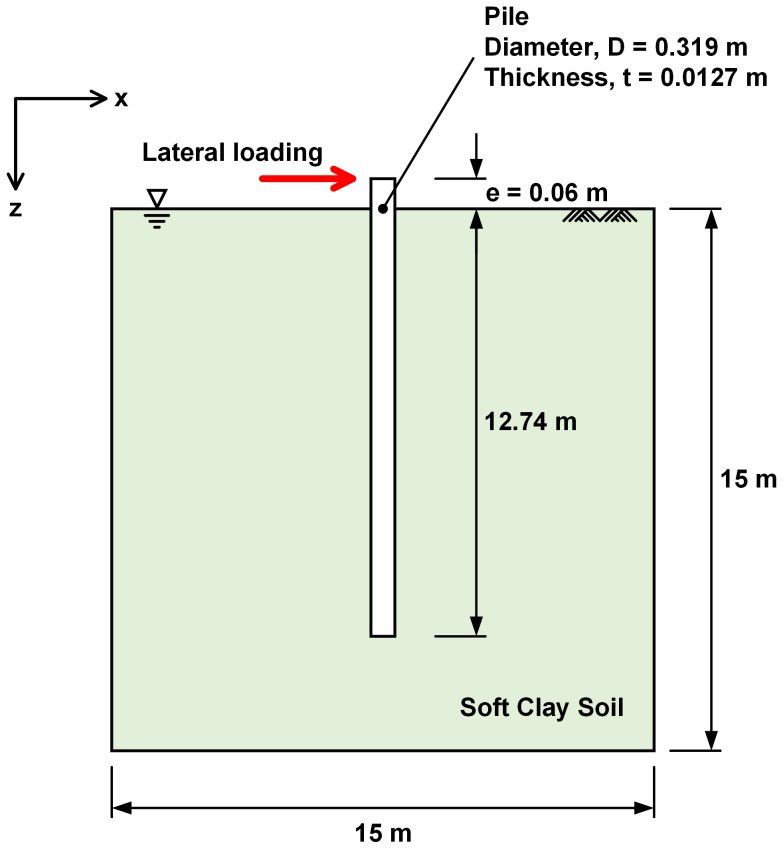

Figure 9. Geometry for FE analysis with Cam-Clay model (Lin et al. 2014)

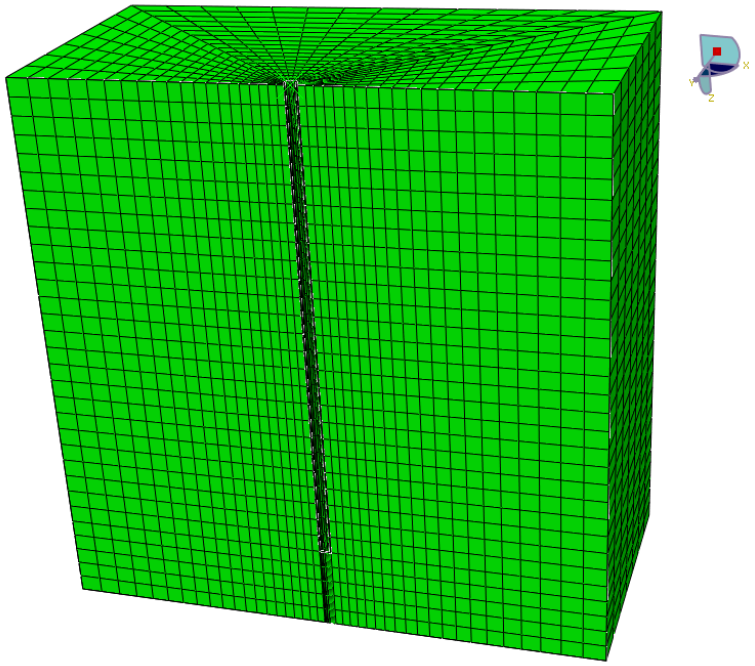

Figure 10. Laterally loaded pile modeling with Cam-Clay model by ABAQUS

3.4.2 Material and Interface Properties

Cam-Clay model is applied for soft clay, and a pile is modeled by Linear-Elastic model. Material and interface properties are summarized in **Table 3** and **Table 4**. Material properties are based on Lin et al. (2014). Several unknown parameters, such as shear modulus, G, stress ratio, M, OCR, and permeability, k, would be calibrated using the trial-error method. Lin et al. (2014) do not mention interface elements and properties in Lin's numerical analysis, but Lin et al. (2016) mention that the interface stiffness would be high to minimize interpenetrating between soil and a pile. Based on the calibration for the interface properties, the best fit shown in the solid line to the existing literature when the value of tangential behavior, μ, is equal to 0.9 for ABAQUS finite element analysis.

Table 3. Material properties for FE analysis with Cam-Clay model (Lin et al. 2014)

Material Parameters	**Soil**	**Pile**
Model	Cam-Clay	Linear-Elastic
Density, ρ (kg/m^3)	2000	7850
Young's Modulus, E (MPa)	-	218,000
Poisson's Ratio, v	-	0.3
Shear Modulus, G (MPa)	10	-
Slope of unloading-reloading line, κ	0.033	-
Slope of normal compression line, λ	0.165	-
Stress ratio, M	1.2	-
OCR	2	-
Friction Angle, ϕ (°)	20	-
Permeability, k (m/s)	1e-10	-
Void Ratio, e	1.64	-

Table 4. Interface properties for FE analysis with Cam-Clay model

Interface Properties	
Tangential Behavior	0.9
Normal Behavior	"Hard" Contact

3.4.3 Results of FE Analysis

Figure 11 shows the lateral load vs. pile deflection curve comparing ABAQUS results and Matlock's result. ABAQUS results show the good agreement with Matlock (1970). These good-matched results show that some unknown properties, in particular interface properties, are well-calibrated. All calibrated material and interface properties would be used to the numerical analysis of the laterally loaded pile under scour condition in the CHAPTER 4.

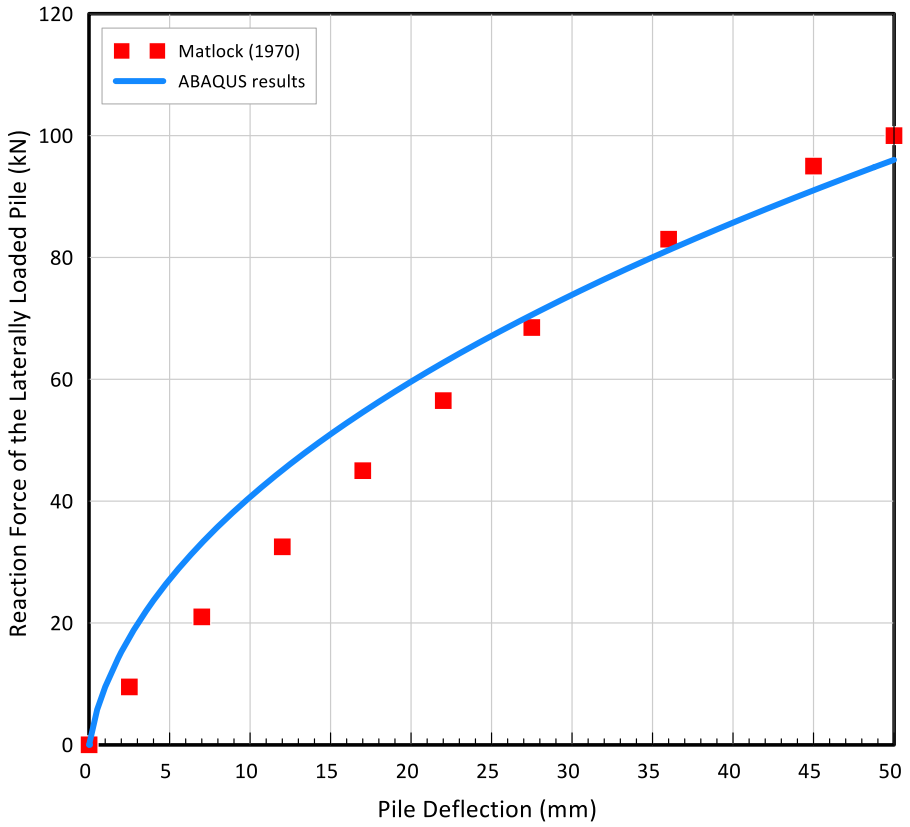

Figure 11. Lateral Load vs. Pile Deflection curve compared ABAQUS results to Matlock (1970)

3.5 Summary

In this chapter, the 3-dimensional laterally loaded pile FE analysis without scour condition is conducted using by ABAQUS. Two constitutive models are pertained: Mohr-Coulomb model and Cam-Clay model. Some unknown material and interface properties are calibrated through trial-and-error method. These unknown material and interface properties, which are obtained from the calibration, would be used for the laterally loaded pile analysis under scour condition. The laterally loaded pile analysis under scour condition also would be explained in the next CHAPTER 4.

CHAPTER 4. LATERALLY LOADED PILE MODELING WITH SCOUR CONDITION

4.1 Introduction

The laterally loaded pile analysis without scour condition is completed in the previous CHAPTER 3. Next, the 3-dimensional laterally loaded pile analysis under scour condition would be carried out in this CHAPTER 4. ABAQUS also would be used for the laterally loaded pile finite element analysis in this chapter. The geometry would be changed depending on scour depth, scour width, and scour slope angle. Material and interface properties of soil and a pile are based on calibration results in the previous chapter. Initial, loading, and boundary conditions are as same as the ones which are mentioned in the previous chapter. There is one difference between the previous modeling in CHAPTER 3 and the current modeling in CHAPTER 4: one additional step, model change, to model the scour condition depending on time, *t*. Results of pile responses under the lateral load and plastic deformation depending on scour geometry would be described in this chapter.

4.2 Laterally Loaded Pile Modeling with Scour Condition using ABAQUS

In the same manner as the laterally loaded pile analysis without scour condition, the same step, load, and boundary conditions are applied for the laterally loaded pile numerical modeling with scour condition, and these conditions are already explained in the previous chapter. The same interface elements and properties in the previous chapter are applied. The differences between non-scour and scour condition are adding scour geometry, such as scour depth, width, and slope angle,

and one additional step, which would be called model change step, using keyword *MODEL CHANGE.

The laterally loaded pile modeling with scour condition assumes that scour has already been stable, and the processes of soil deformation and in-situ stress changes have been completed. Because of this reason, this study supposes that there are no more soil deformation and in-situ stress changes when the scour process has been finished, and soil deformation and stress changes due to the lateral load are allowed.

4.2.1 Scour Geometry

Scour effect can explain the geometry changes due to the fluid flow depending on time, t. Further, in real scour condition, the scour width, S_w, is not infinite, and the scour depth, S_d, and the slope angle, α, would be also considered. Therefore, in this study, there are three main parameters to model the laterally loaded pile finite element analysis under scour condition: scour depth, S_d, scour width, S_w, and scour slope angle, α. **Figure 12** is the geometry of the pile analysis under scour condition. Different scour depth, S_d, width, S_w, and slope angle, α, would be considered for the laterally loaded pile numerical analysis under the scour condition.

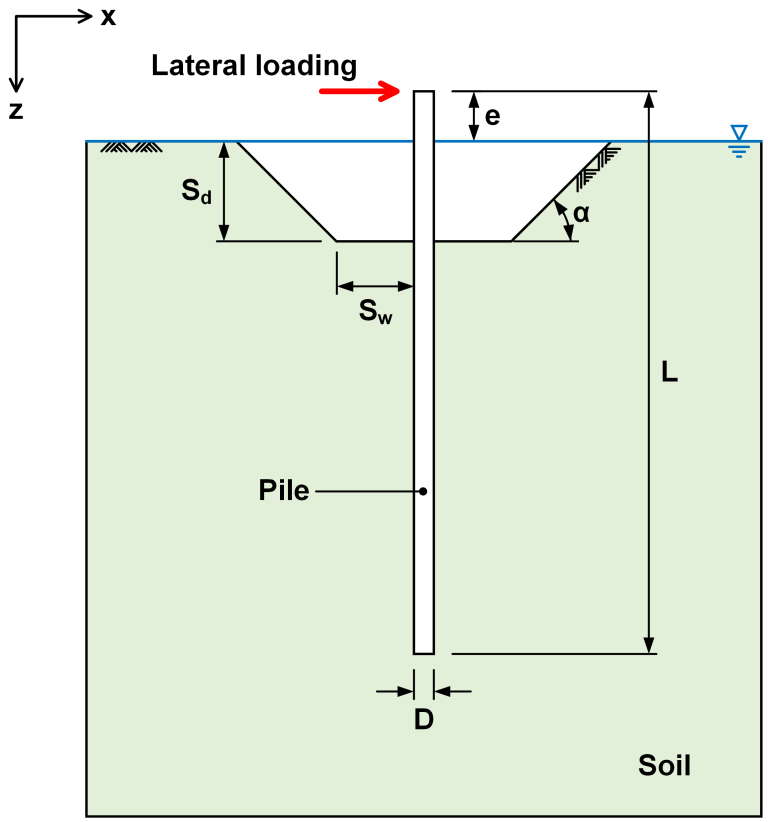

Figure 12. The geometry of pile deflection analysis with scour depth, S_d, width, S_w, and angle, α

4.2.2 Numerical Analysis Procedure of the Laterally Loaded Pile Analysis

There are four steps of the laterally loaded pile numerical analysis under the scour condition. One difference compared with the previous pile numerical modeling is that one additional step using keyword *MODEL CHANGE is added in between initial and geostatic steps. Details of the pile analysis procedure with scour condition are shown as **Figure 13**. Keyword *MODEL CHANGE would be described in the next section 4.2.3.

This study supposes that no more soil deformation and in-situ stress changes due to the soil loss allow when the scour process has been finished. For this reason, in the model change step, a sufficiently large amount of time would be applied to complete the consolidation effect, i.e., soil

deformation (rebound behavior) and in-situ stress changes, which is generated by scour geometry removal. After the model change step, the geostatic step would revalidate initial stress equilibrium, horizontal and vertical in-situ stresses, with pore water pressure after geometry changes. No more deformation due to the consolidation effect is allowed in the geostatic step. Additional soil deformation and stress changes would appear when the lateral load on the pile head is applied

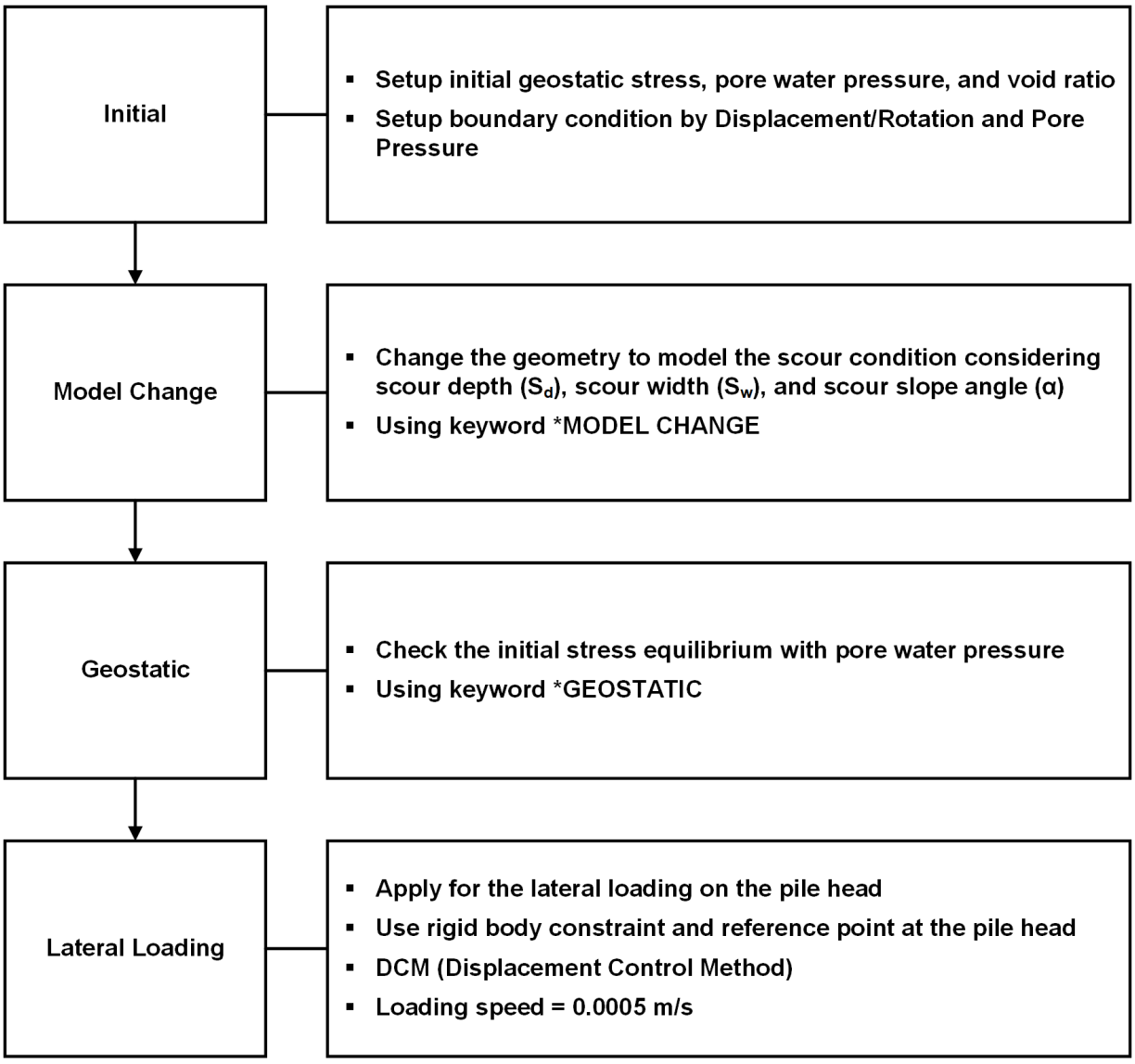

Figure 13. The procedure of the laterally loaded pile FE analysis with the scour condition

4.2.3 Keyword, *MODEL CHANGE

It is hard to define initial stresses, especially the horizontal stress, on the uneven surface, for example slope geometry in ABAQUS (see **Figure 12**). This issue may be solved when User-Subroutine for initial stresses, SIGINI, is used. Bubel et al (2012 and 2012) choose User-Subroutine, SIGINI, to set the initial stress state on the slope foundation. Therefore, User-Subroutine, SIGINI, may be used to establish the exact initial in-situ stress on the uneven surface.

Scour is soil loss due to the fluid flow. This means that the geometry and stress distribution would be changed with respect to time, *t*. ABAQUS provides one of the tools for the geometry change due to soil loss with fluid flow with respect to time, *t*, which is the keyword *MODEL CHANGE. The keyword *MODEL CHANGE allows geometry changes during the analysis procedure depending on step and time, *t*. He et al (2019), Jia et al (2022), and Chavan et al (2022) choose the keyword *MODEL CHANGE for establishing stress history depending on the geometry change.

As shown in **Figure 14**, scour mudline with a specific scour depth, width, and slope angle would be set up for a part of scour geometry in the initial step. In the initial step, the part of scour geometry is not removed. After the initial step, ABAQUS keyword *MODEL CHANGE is applied in the model change step. In the model change step, the part of scour geometry is deleted to anticipate in-situ stress changes and soil deformation due to the unloading process. This unloading process makes time-dependent changes of in-situ stress and soil deformation. For this reason, a sufficiently large amount of time would be required to stabilized in-situ stress and soil deformation. 200 days is adopted in this model.

Therefore, the keyword *MODEL CHANGE can be used to establish the geometry and stress distribution (or stress history) changes depending on time, *t*. In this study, the keyword

*MODEL CHANGE would be used to model the scour effect. The keyword *MODEL CHANGE would be in between the initial step and the geostatic step.

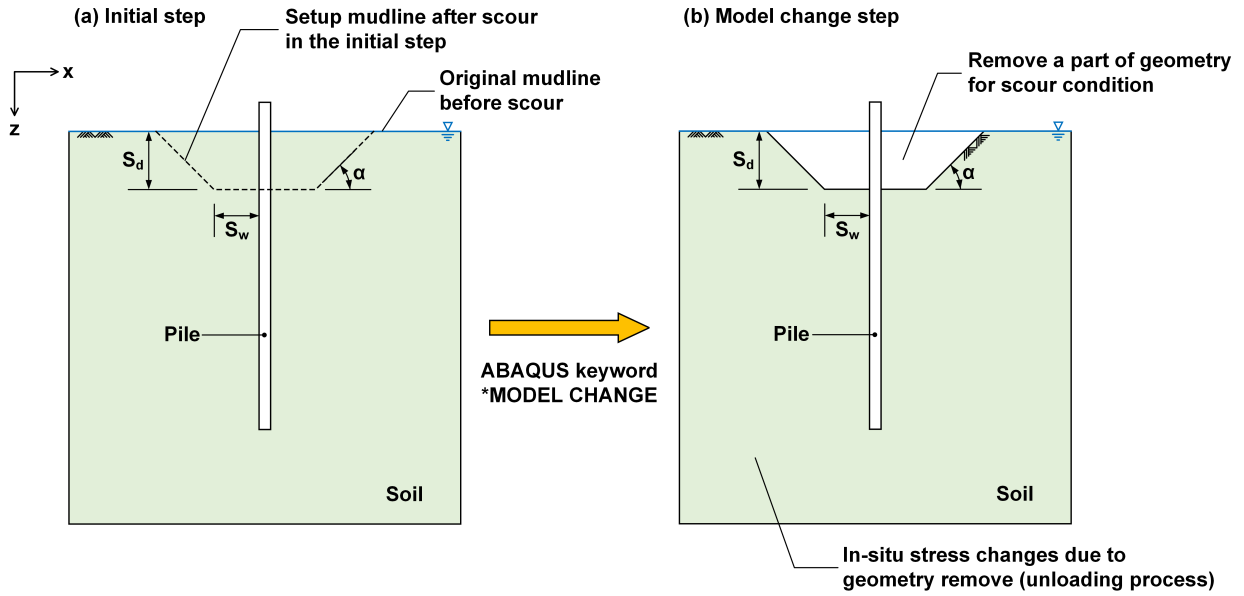

Figure 14. The process of ABAQUS keyword *MODEL CHANGE

4.3 Plastic Deformation/Strain Distribution depending on Scour Geometry

Plastic deformation results would be described depending on the scour geometry, scour depth, width, and angle using PE which means the plastic strain in this chapter. PE is the tensor measurement. Further, the plastic strain is increased depending on the pile deflection.

Zania et al. (2012) describe the plastic minimum principal strain contours with respect to the laterally loaded pile analysis depending on the pile diameter. According to the paper by Zania et al. (2012), the main failure zone is induced by the lateral load at the passive side of the pile along the direction of the lateral load (see **Figure 16 (a)**). Moreover, another failure zone is also

generated by the free-standing soil at the active side of the pile, not by the lateral load. The free-standing soil can be shown due to the gap between a pile and soil to which the lateral load leads.

Figure 15 is ABAQUS PE, Max. Principal results in the non-scour effect based on both Li et al. (2013) and Lin et al. (2014). As Zania et al. (2012) mention, ABAQUS shows the plastic strain in both passive and active sides of the pile. The main plastic strain is shown in the passive side of the pile due to the lateral load. Further, as shown in **Figure 15 (c) and (d)**, the plastic strain can be shown in the back side of the pile (the active side of the pile). This plastic strain can be generated by the free-standing soil deformation (see **Figure 16 (b)**).

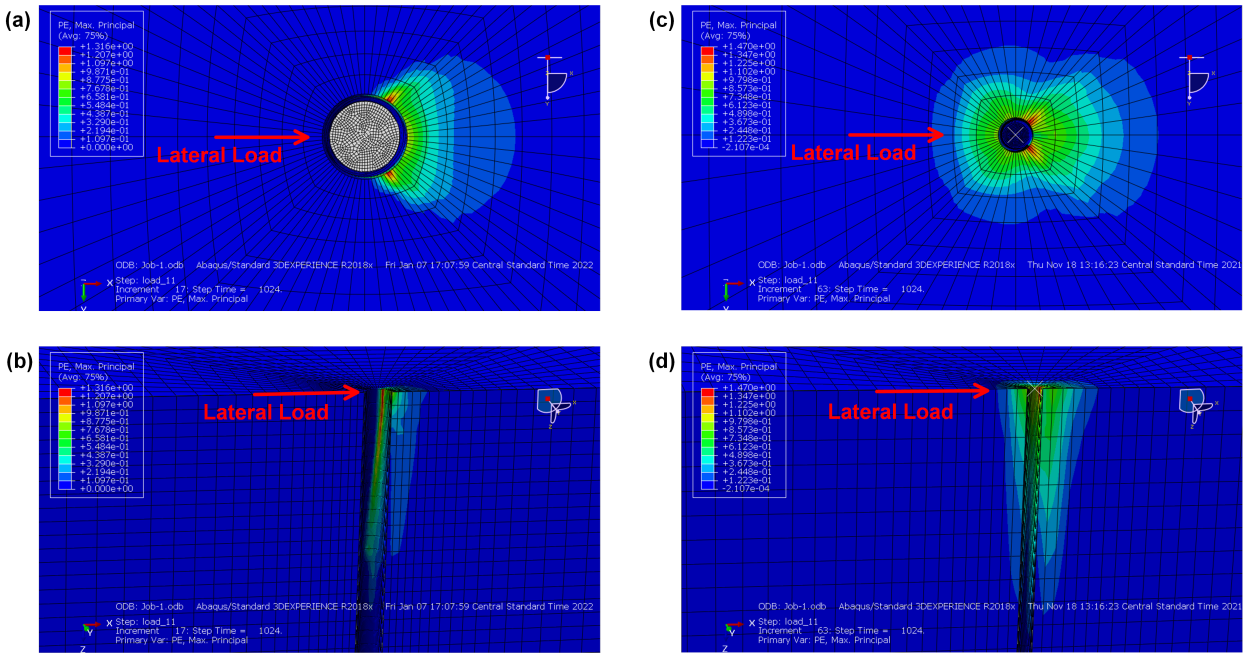

Figure 15. PE results at pile deflection = 512 mm with non-scour condition: (a) and (b) Li et al, 2013, (c) and (d) Lin et al, 2014

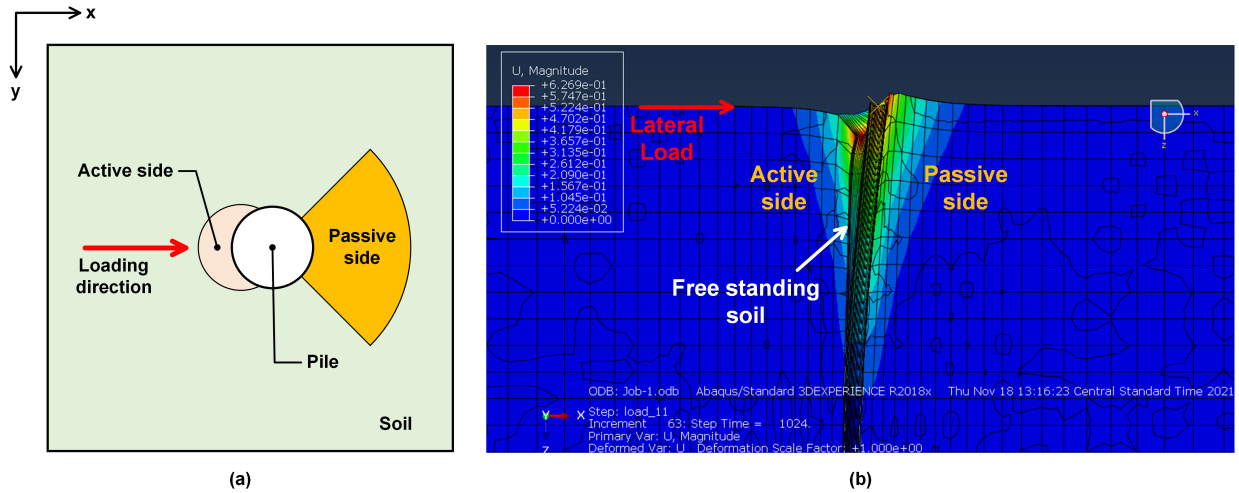

Figure 16. (a) Outline of plastic deformation due to the lateral load, (b) Soil deformation results (Lin et al, 2014)

4.4 Numerical Modeling with Mohr-Coulomb Model

4.4.1 Parametric Case of Geometry

The parametric study of the laterally loaded pile under the scour condition would be performed depending on different scour depth, S_d, scour width, S_w, and scour slope angle, α, to consider scour. This parametric study is also based on Kim et al. (2011) and Li et al. (2013). The boundary dimension of soil and a pile is shown in section 3.3.1. Material and interface properties are shown in **Table 1** and **Table 2** at the section 3.3.2.

4.4.2 Laterally Loaded Pile Response depending on Scour Depth, S_d

The laterally loaded pile analysis would be performed depending on different scour depths, S_d. For Mohr-Coulomb model, there are 5 layers as shown in **Figure 6**, and the scour depth, S_d, would be confined within the upper marine clay. For this reason, 4 cases of scour depth, as 1D, 2D, 4D, and 6D, are applied for comparing with non-scour case, and there is still remaining upper

clay soil even for the extreme case of S_d = 6D. The pile diameter, D, is 1.016 m. Scour width, S_w, is infinite, and scour slope angle, α, is not considered.

The reaction force of the laterally loaded pile vs. pile deflection curves depending on the scour depth, S_d, are as shown in **Figure 17**. Soil which supports the pile is removed due to the scour effect, and this soil loss makes the reaction force decrease when the scour depth is increased (Li et al, 2013). For example, the reaction force in the non-scour case is around 50 % higher than the force when scour depth, S_d, is 6 D.

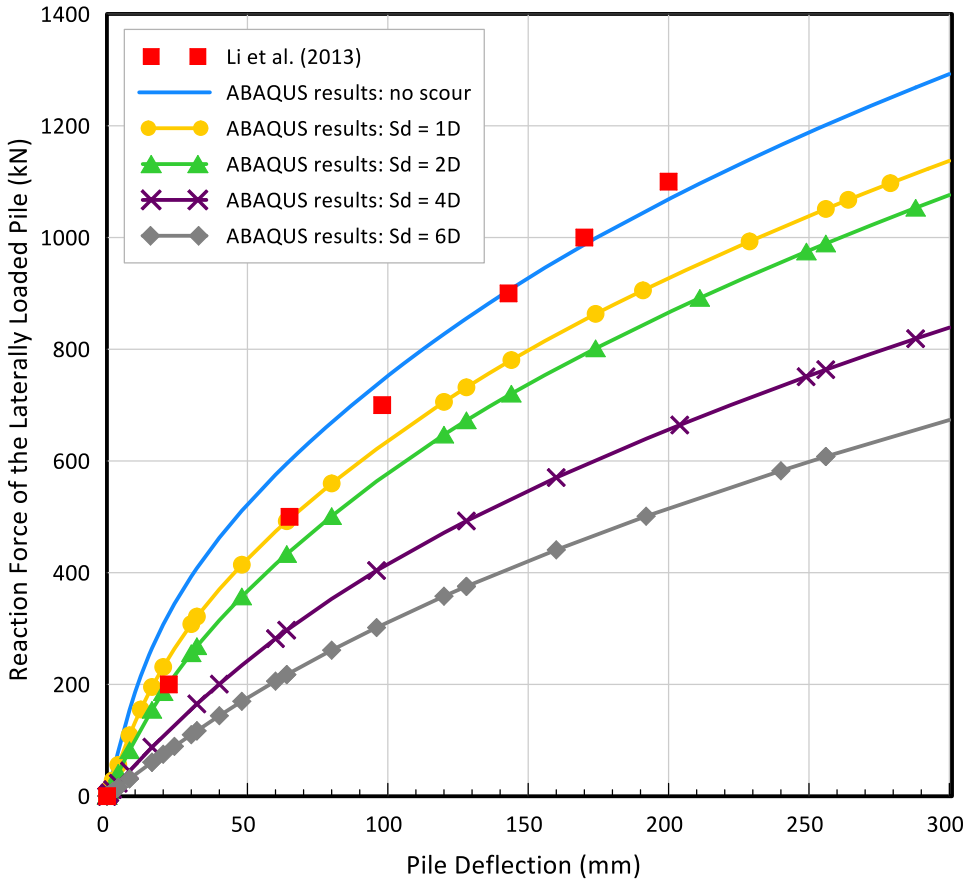

Figure 17. Lateral load vs. Pile deflection curve depending on the scour depth, S_d, with Mohr-Coulomb Model

Figure 18 is the maximum principal plastic strain (PE) results depending on the scour depth at the pile deflection is equal to 256 mm. The main PE is induced in the passive side of the pile. The PE is also decreased when the scour depth is increased. Non-scour, 1D, and 2D cases cannot see the PE at the active side of the pile, but the PE in 4D and 6D cases appears at the active side of the pile because the free-standing soil at the active side of the pile is deformed.

S_d	x-z coordinate	x-y coordinate
0D (no scour)	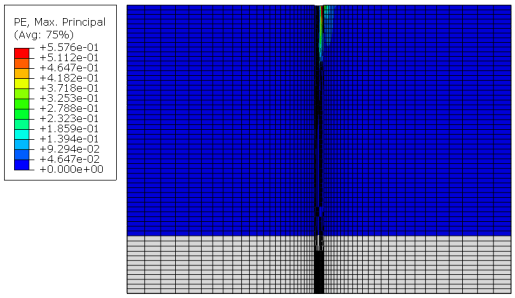	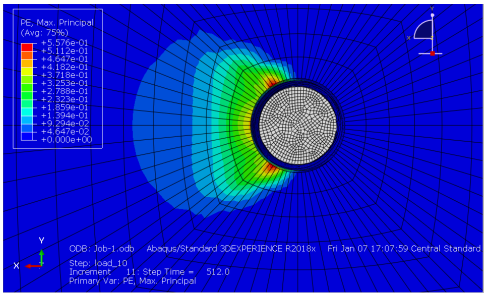
1D	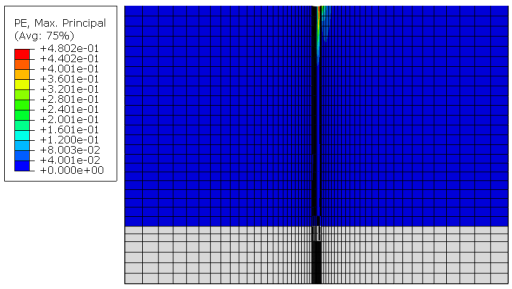	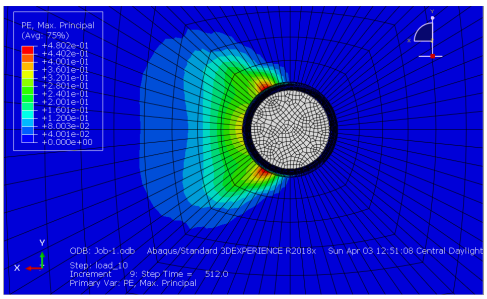
2D	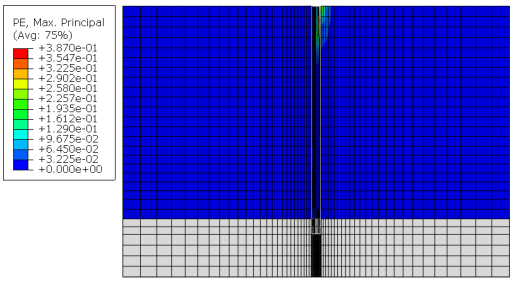	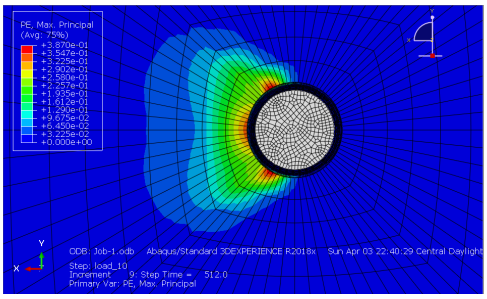
4D	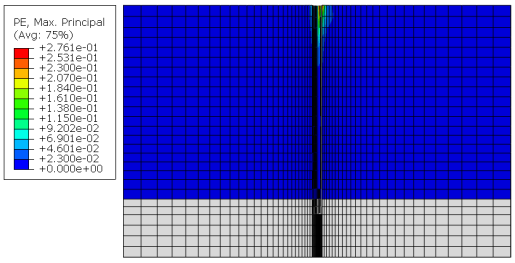	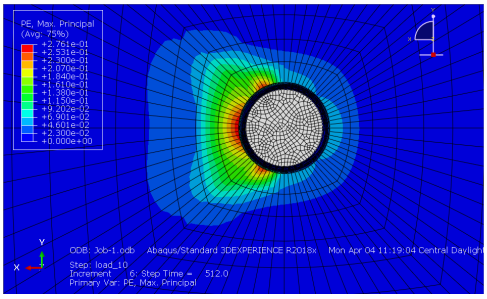
6D	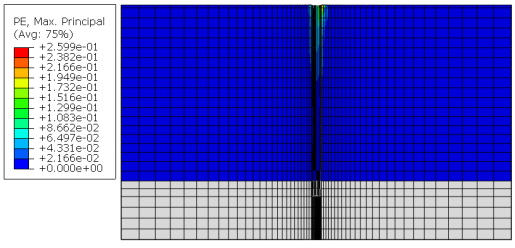	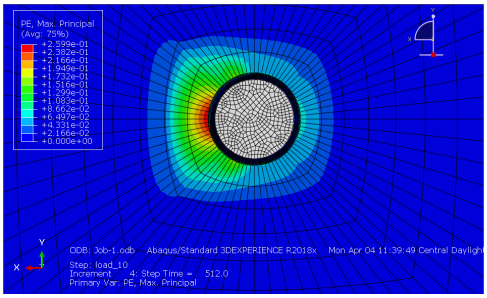

Figure 18. Plastic strain, PE, results depending on scour depth, S_d, at pile deflection = 256 mm

4.4.3 Laterally Loaded Pile Response depending on Scour Width, S_w

The laterally loaded pile FE analysis would be performed depending on different scour widths, S_w. There are 6 cases of scour width: 0 m, 0.5 m, 1 m, 2 m, 4 m, and infinite. Scour depth, S_d, is fixed, and 4D is chosen in this pile deflection FE analysis. Scour angle, α, is also fixed, and 26 ° which is a natural slope to be stable is applied (Li et al, 2013).

As shown **Figure 19**, the reaction force of the laterally loaded pile is decreased when scour width is increased. In particular, once the scour width reaches to 2 m, the reaction force results between 2 m scour width and the infinite scour width are not much different (see **Figure 20**). Further, the decreased reaction force is around 20 % when the scour width varies from 0 m to 4 m and infinite scour width.

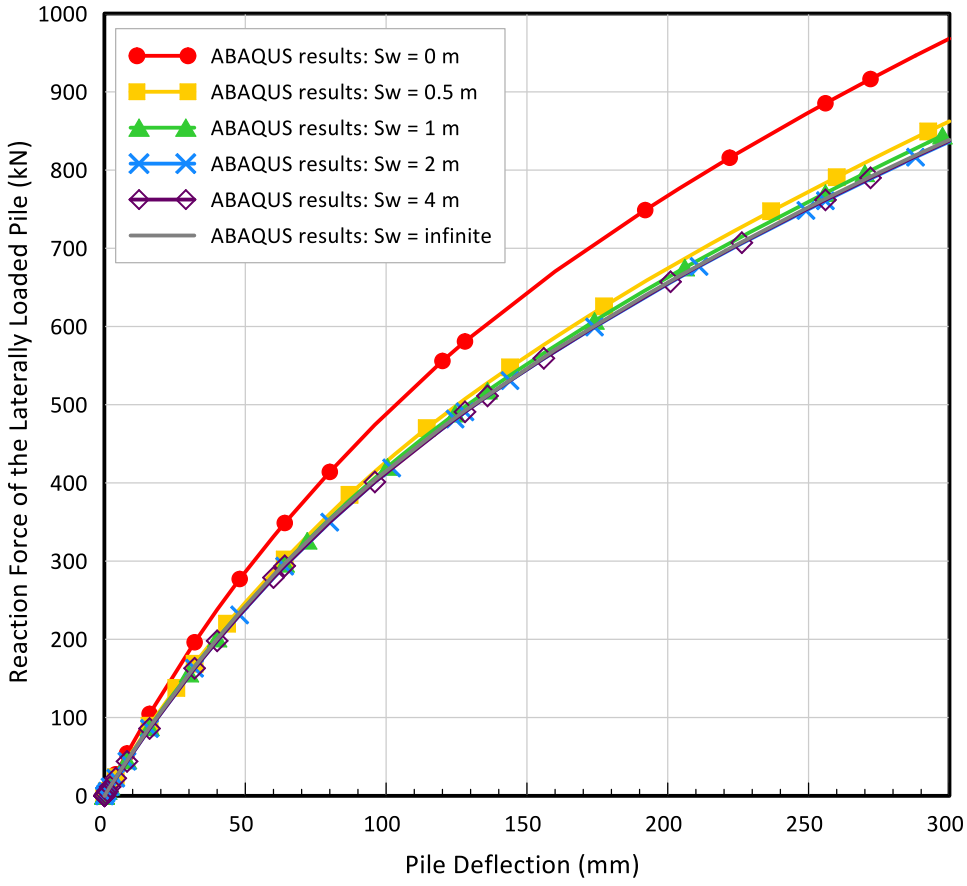

Figure 19. Lateral load vs. Pile deflection curve depending on the scour width, S_w, with Mohr-Coulomb Model

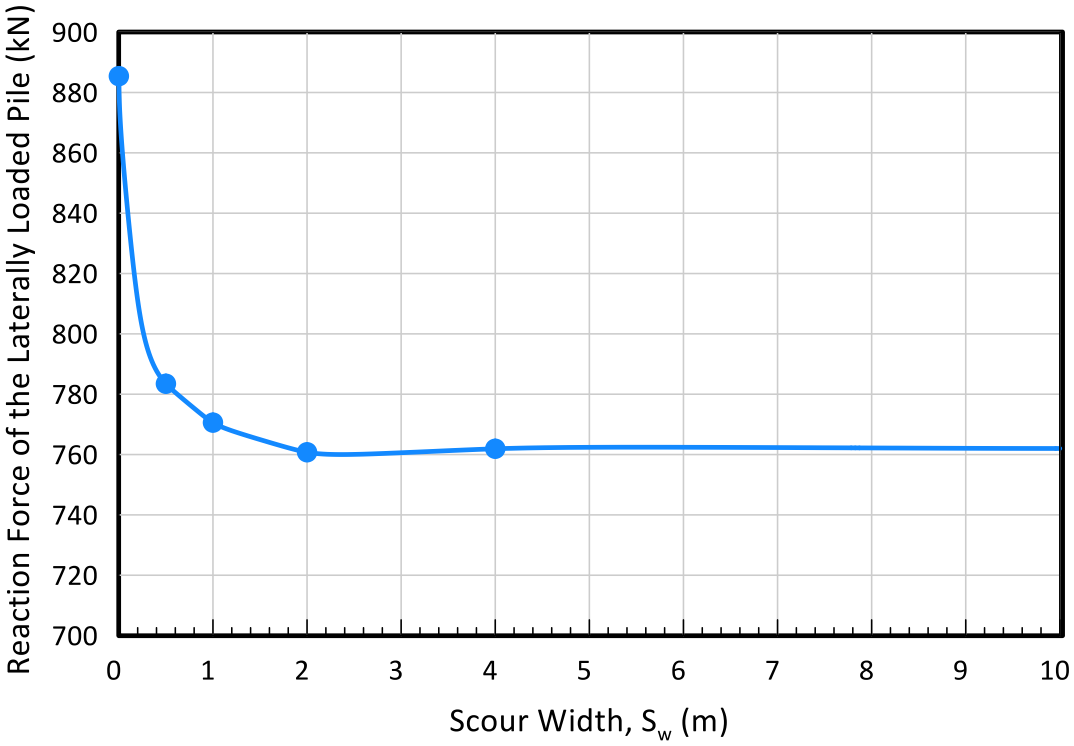

Figure 20. Reaction force distribution depending on scour width, S_w, at the pile deflection = 0.256 m with Mohr-Coulomb Model

Figure 21 is the maximum principal plastic strain (PE) results depending on the scour width at the pile deflection is equal to 256 mm. Based on the PE results, it seems that plastic deformation can be expanded at scour slope when scour width is 0 m. Further, the plastic deformation can be expanded near the edge of the scour width geometry when scour width is 0.5 m to 2 m. However, the plastic deformation shape when the scour width is 4 m would be similar to the one when the scour width is infinite.

S_w	x-z coordinate	x-y coordinate
0 m	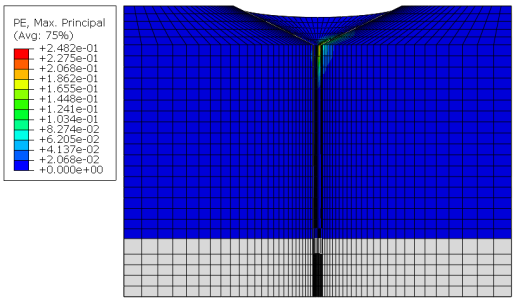	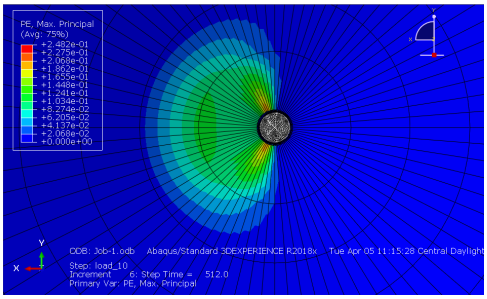
0.5 m	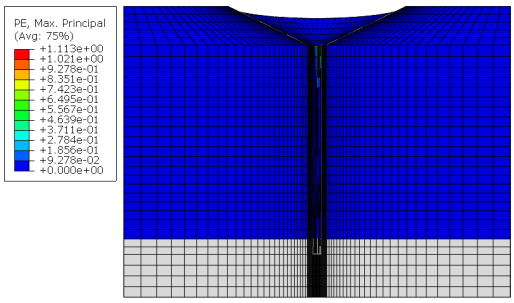	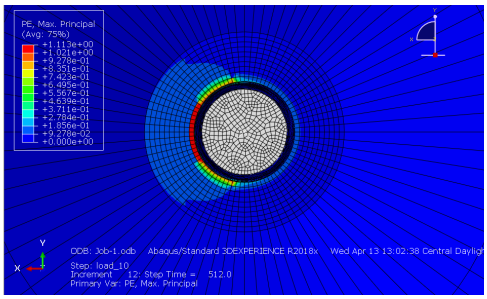
1 m	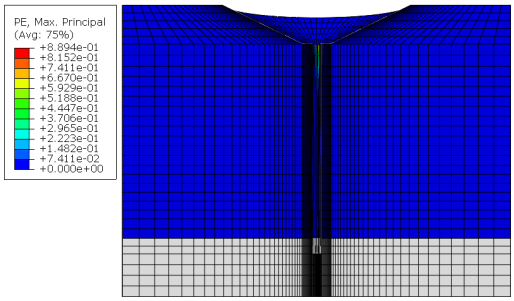	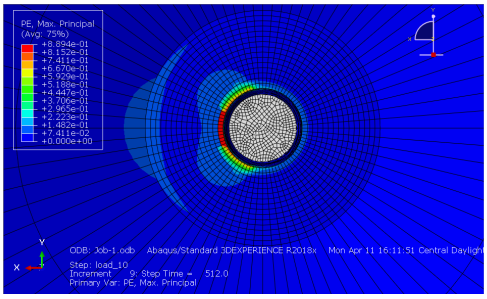
2 m	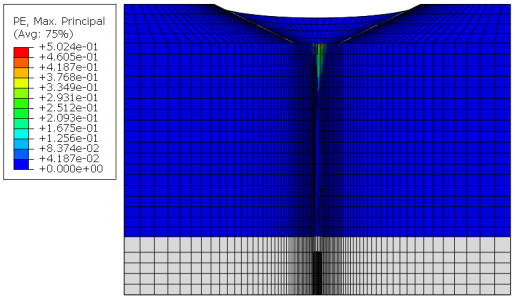	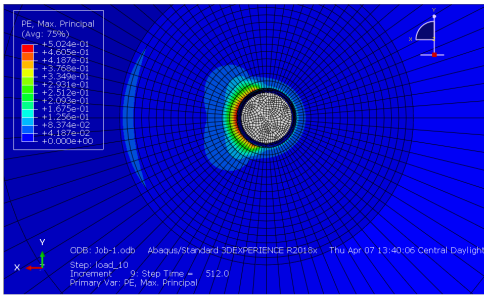
4 m	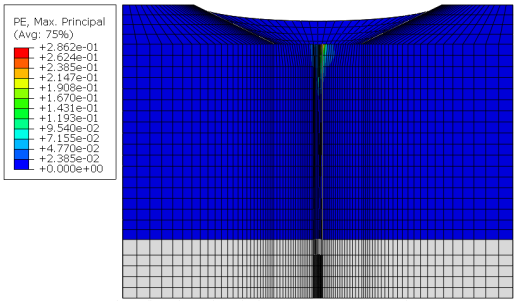	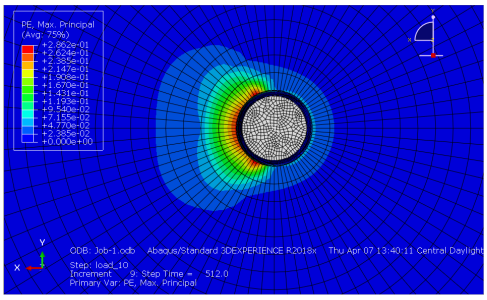

Figure 21. Plastic strain, PE, results depending on scour width, S_w, at pile deflection = 256 mm

4.4.4 Laterally Loaded Pile Response depending on Scour Angle, α

In this section, the key parameter of the laterally loaded pile FE analysis is scour angle, α. There are 7 cases of the scour slope angle: 90 °, 75 °, 60 °, 45 °, 26 °, 13 °, and 0 °. There are the fixed 4D in scour depth is used. The fixed value of 0.5 m is chosen for the scour width, S_w.

As shown **Figure 22**, the reaction force of the laterally loaded pile is gradually decreased, and the reaction force results at the scour slope angle is equal to between 13 ° and 0 ° show similar results, and this means that the lateral reaction force is converged when the scour slope angle is equal to 13 °. Further, the decreased reaction force is around 8 % when the scour slope angle varies from 90 ° to 13 ° and 0 ° (see **Figure 23**).

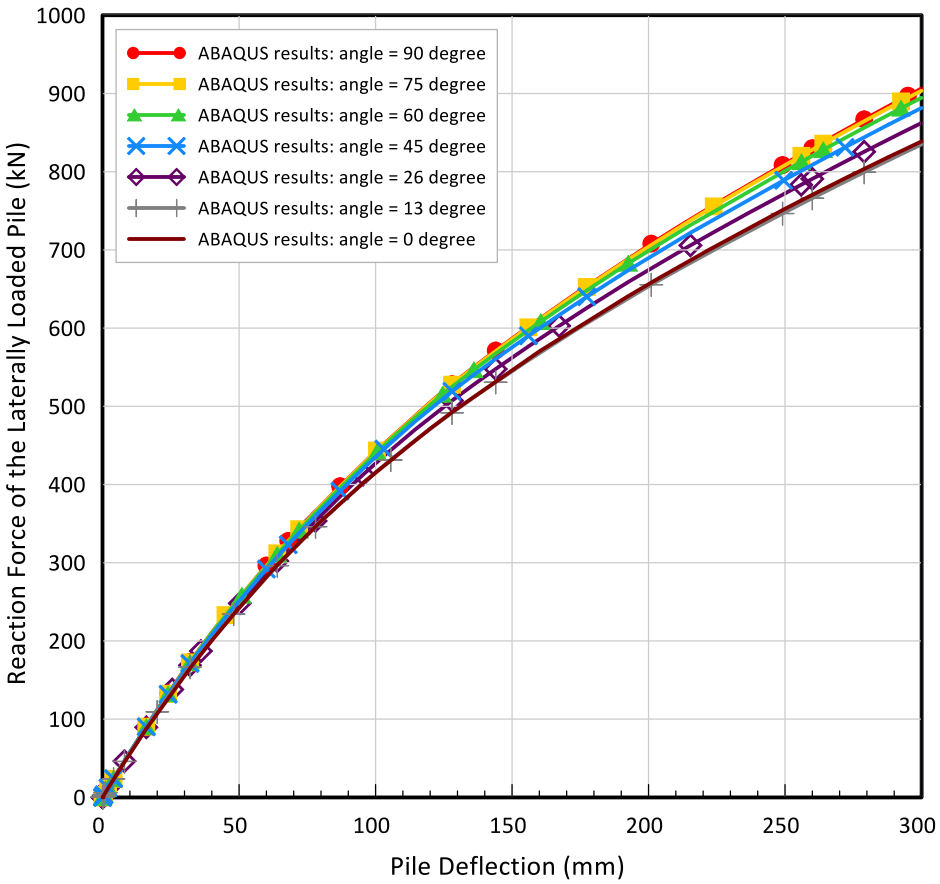

Figure 22. Lateral load vs. Pile deflection curve depending on the scour slope angle, α, with Mohr-Coulomb Model

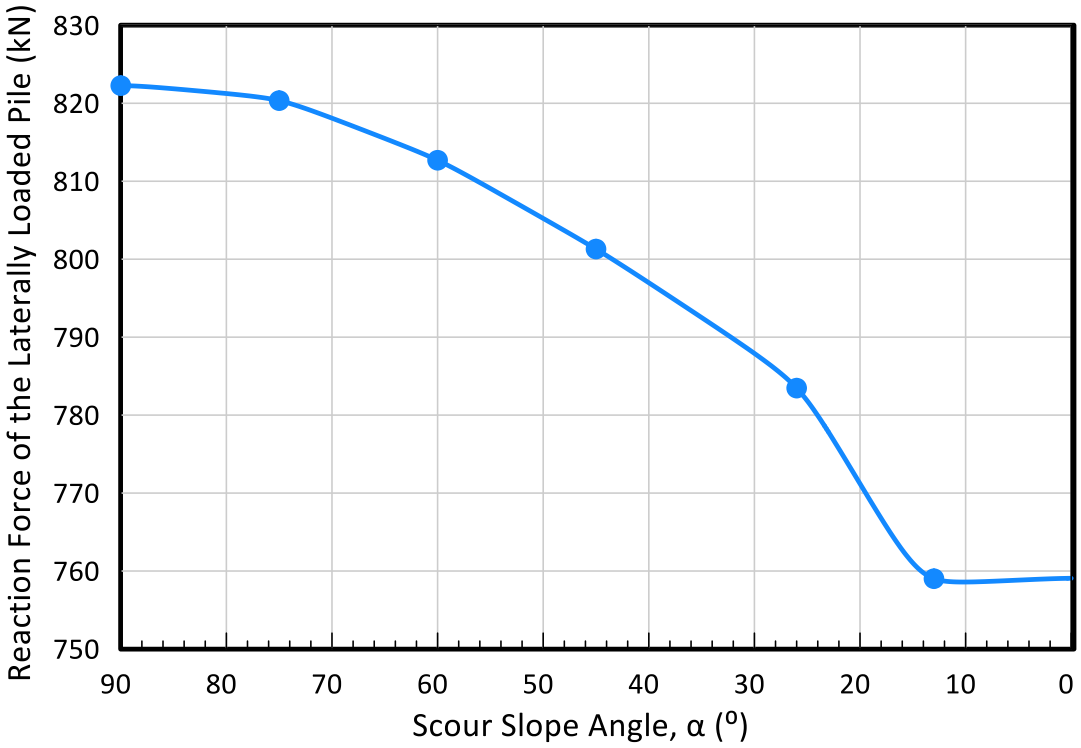

Figure 23. Reaction force distribution depending on scour slope angle, α, at the pile deflection = 0.256 m with Mohr-Coulomb Model

Figure 24 is the maximum principal plastic strain (PE) results depending on the scour slope angle at the pile deflection is equal to 256 mm. When the scour slope angle is 90 °, the high PE appears at the edge of the scour width geometry. Then, the PE at the edge of the scour width geometry would be also decreased when the scour slope angle is decreased gently.

α	x-z coordinate	x-y coordinate
90 °	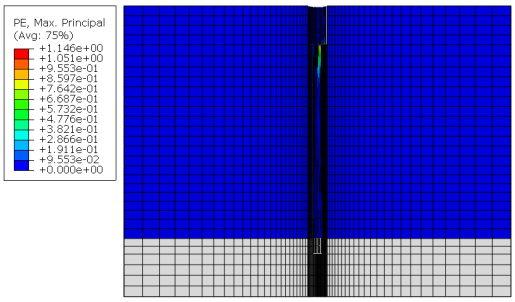	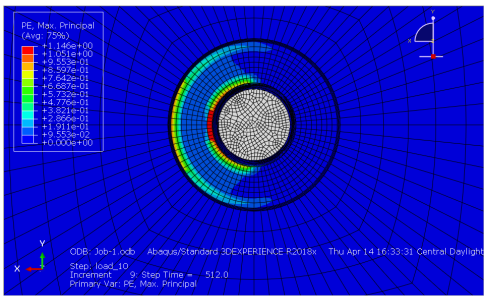
75 °	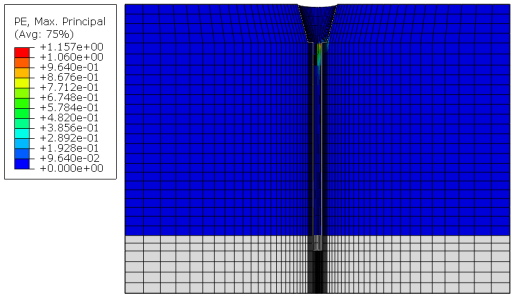	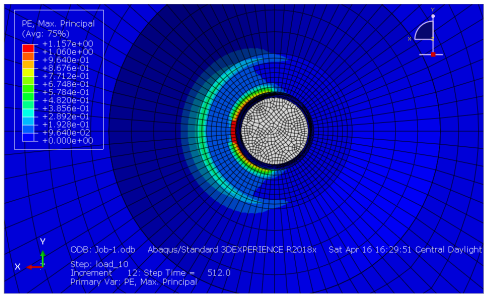
60 °	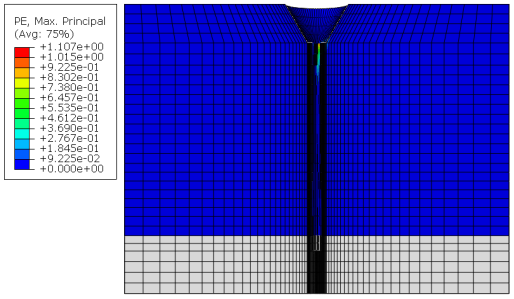	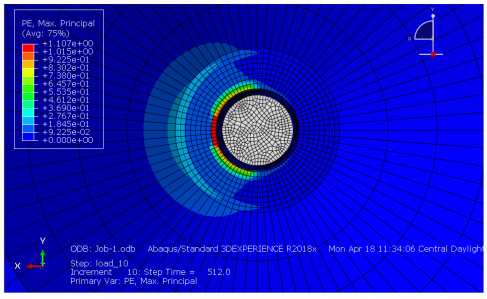
45°	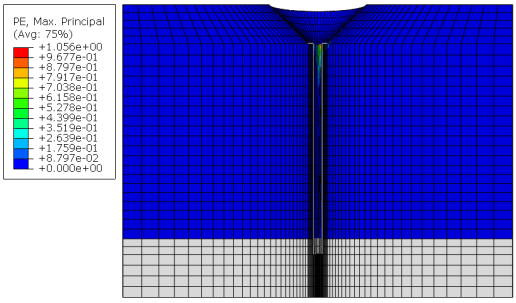	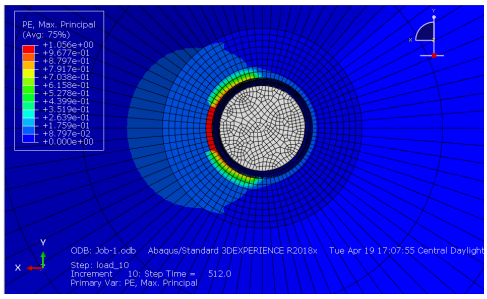
26 °	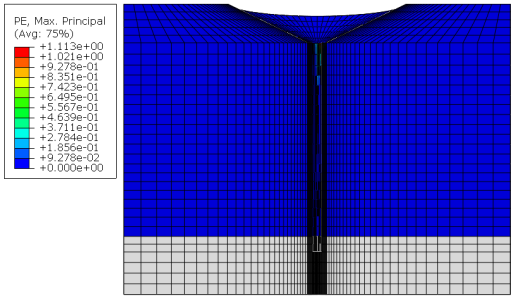	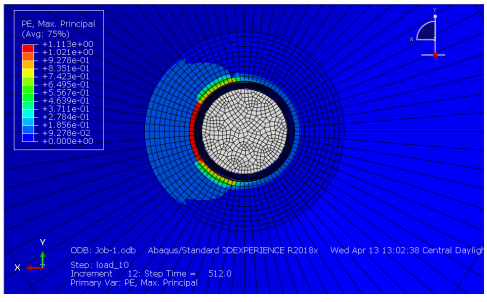

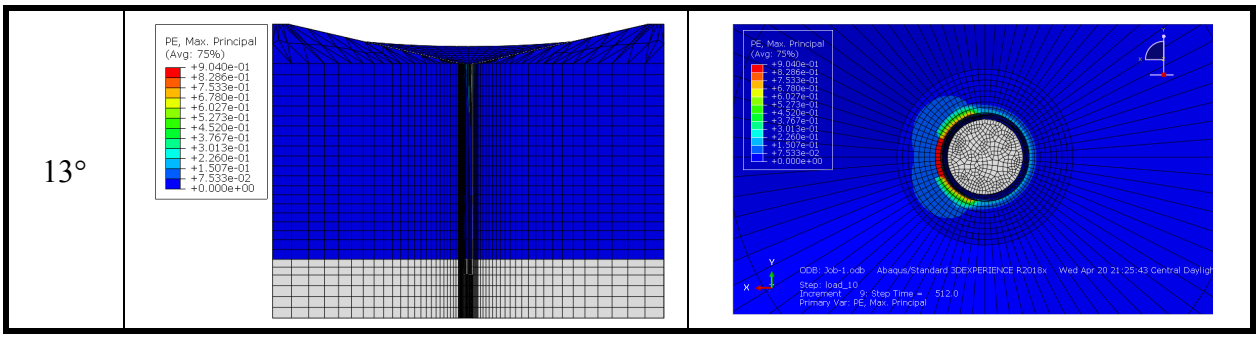

Figure 24. Plastic strain, PE, results depending on scour angle, α, at pile deflection = 256 mm

4.5 Numerical Modeling with Cam-Clay Model

4.5.1 Parametric Case of Geometry

The parametric study of the laterally loaded pile under the scour condition would be performed depending on different scour depth, S_d, scour width, S_w, and scour slope angle, α, to consider scour. This parametric study is also based on Lin et al (2014) and Lin et al (2016). The boundary dimension of soil and a pile is shown in section 3.4.1. Material and interface properties are shown in **Table 3** and **Table 4** at the section 3.4.2.

4.5.2 Results of Pile deflection depending on Scour Depth, S_d

The laterally loaded pile analysis would be performed depending on different scour depths, S_d. There are 4 cases of scour depth: 1D, 3D, 5D, and 8D comparing with no scour effect case. D means the pile diameter which is 0.319 m. In the same manner of Mohr-Coulomb Model, scour width, S_w, is infinite, and scour slope angle, α, is not considered.

The reaction force of the laterally loaded pile vs. pile deflection curves depending on the scour depth, S_d, are as shown in **Figure 25**. When the scour depth is increased, the reaction force of the laterally loaded pile is gradually decreased. Further, at the same manner of Mohr-Coulomb

model, the reaction force in the non-scour case is around 50 % higher than the force when S_d is 8 D.

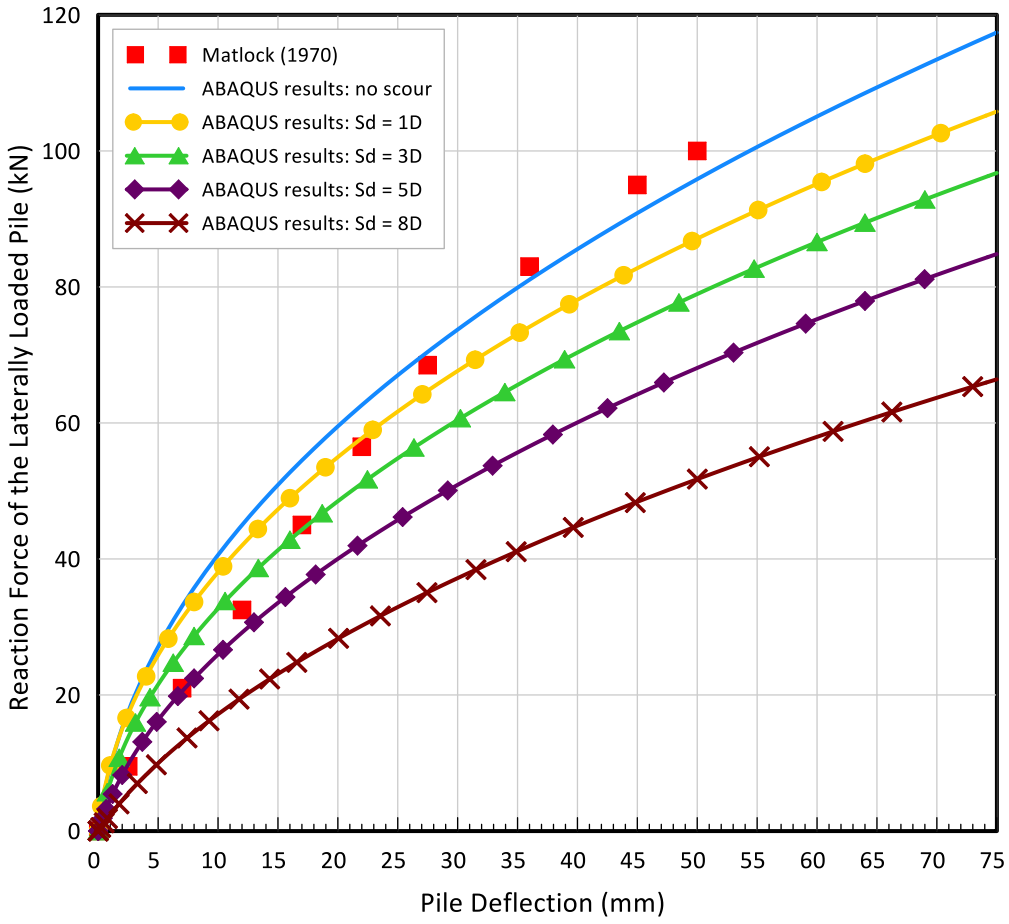

Figure 25. Lateral load vs. Pile deflection curve depending on the scour depth, S_d, with Cam-Clay Model

The maximum principal plastic strain (PE) depending on the scour depth can be shown in **Figure 26**. The maximum PE appears at a node which is located in a certain angle in the x-direction. Further, the PE can be shown along the soil which is contacted with the pile surface. It seems that this PE can be caused by the plastic deformation from the free-standing soil.

S_d	x-z coordinate	x-y coordinate
0D (no scour)	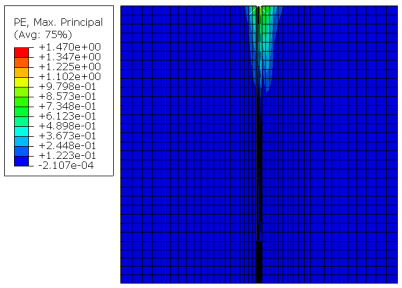	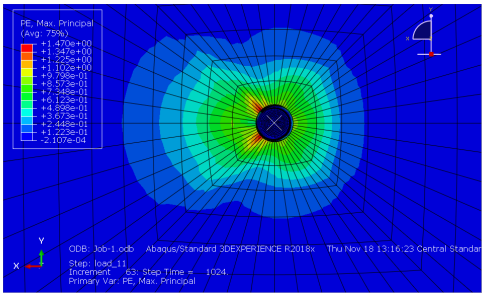
1D	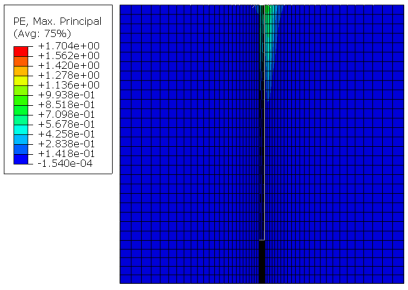	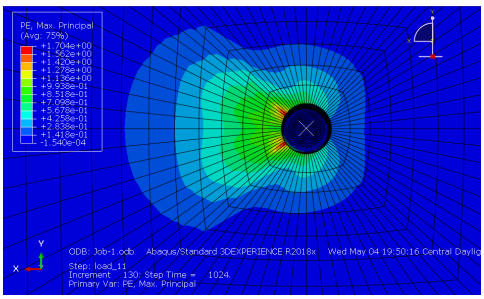
3D	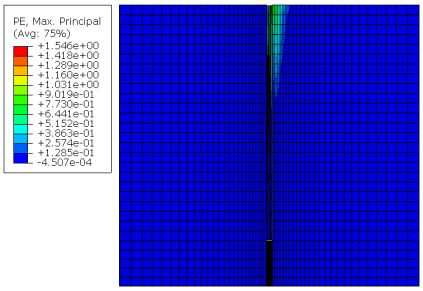	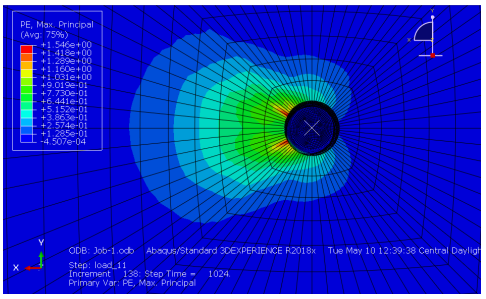
5D	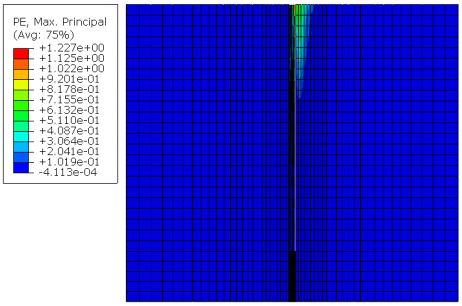	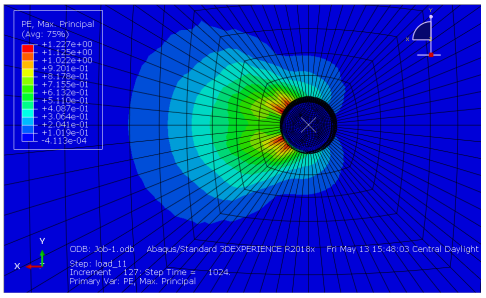
8D	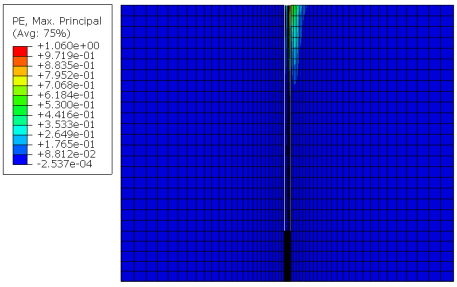	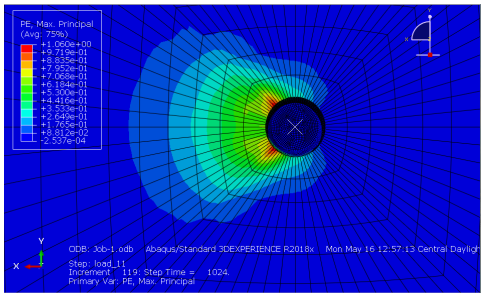

Figure 26. Plastic strain, PE, results depending on scour depth, S_d, at pile deflection = 512 mm

4.5.3 Results of Pile deflection depending on Scour Width, S_w

The laterally loaded pile analysis would be performed depending on different scour widths, S_w. There are 6 cases of scour width: 0 m, 0.5 m, 1 m, 2 m, and infinite. Scour depth, S_d, is fixed, and 5D is used in this pile deflection FE analysis. Scour angle, α, is also fixed, and 40 ° is applied.

As shown **Figure 27**, the reaction force of the laterally loaded pile is decreased when scour width is increased. In particular, once the scour width reaches to 2 m, the reaction force results between 2 m scour width and the infinite scour width are not much different (see **Figure 28**). The amount of decreased reaction force is around 12 % when the scour width varies from 0 m to 2 m and infinite width when the pile deflection is 512 mm.

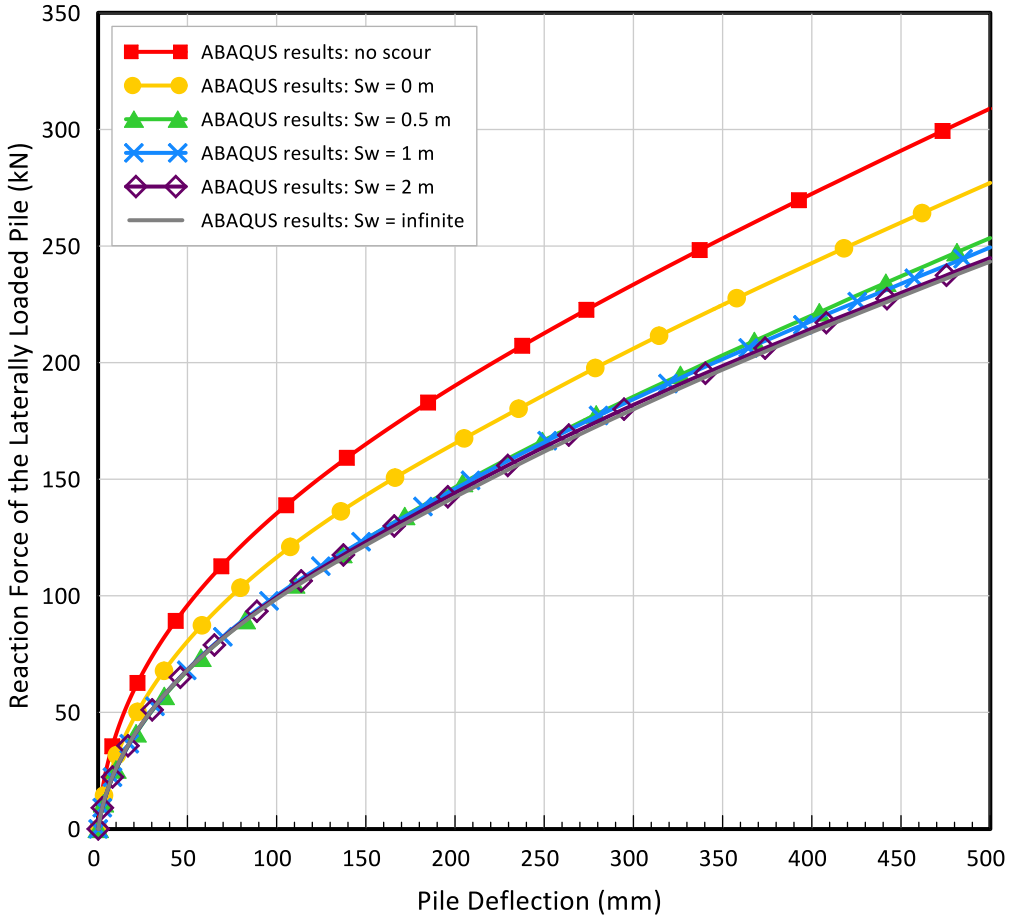

Figure 27. Lateral load vs. Pile deflection curve depending on the scour width, S_w, with Cam Clay Model

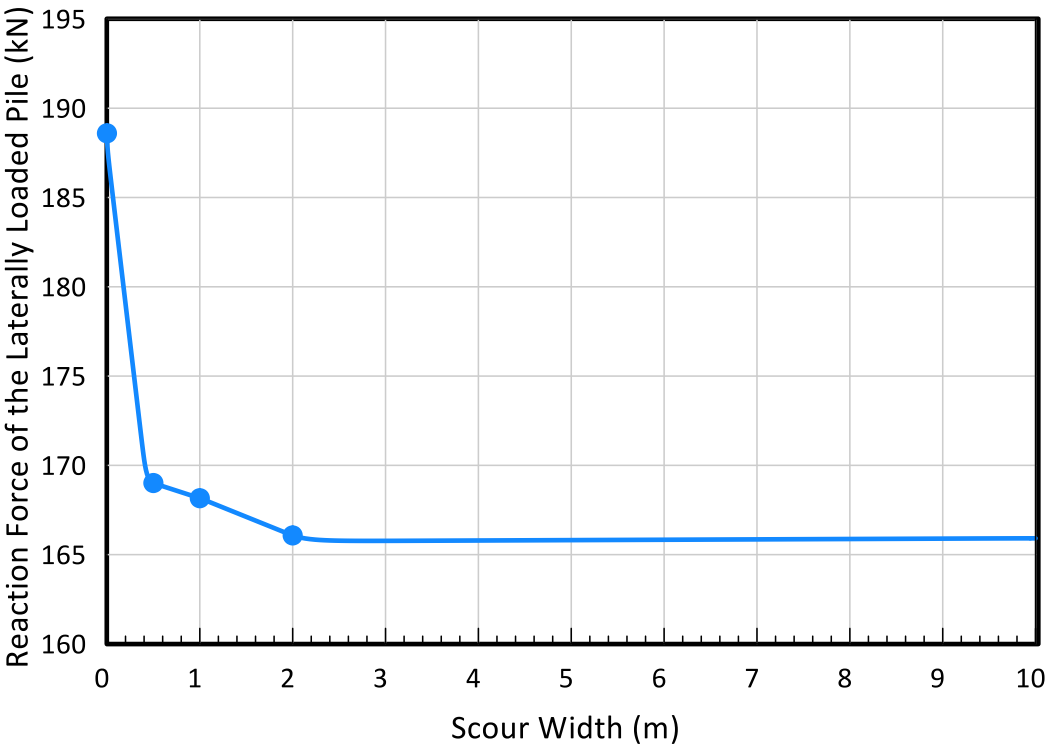

Figure 28. Reaction force distribution depending on scour width, S_w, at the pile deflection = 0.512 m with Cam Clay Model

Figure 29 is the results of the maximum principal plastic strain (PE) depending on the scour width at the pile deflection is equal to 512 mm. The maximum PE also appears at a node which is located in a certain angle in the x-direction as the previous scour depth case study. Based on the PE results, plastic deformation can be expanded at the scour slope when the scour width is 0 m and 0.5 m, and the plastic deformation can be shown near the end of the scour width geometry when the scour width is 1 m. However, the plastic strain/deformation shape when the scour width is 2 m would be similar to the one when the scour width is infinite.

S_w	x-z coordinate	x-y coordinate
0 m	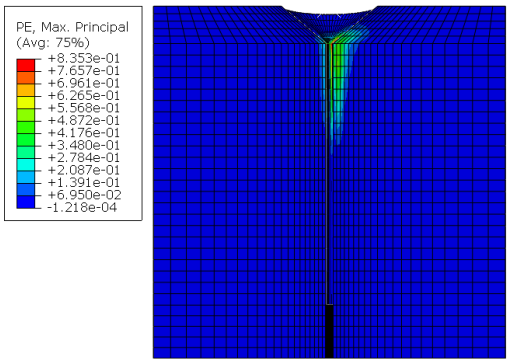	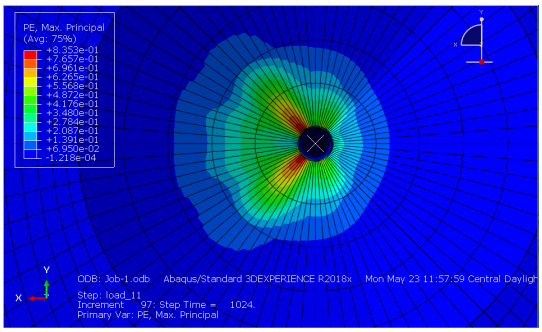
0.5 m	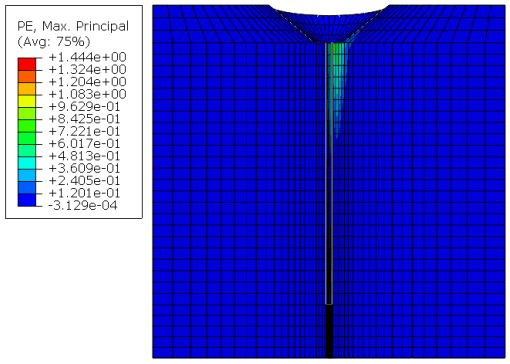	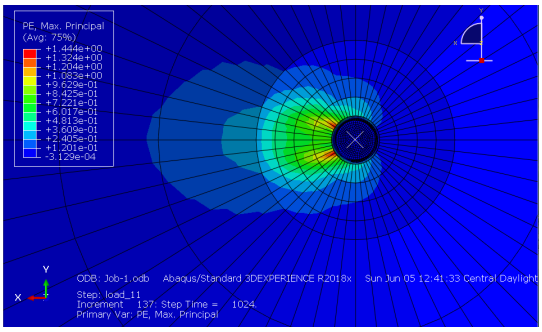
1 m	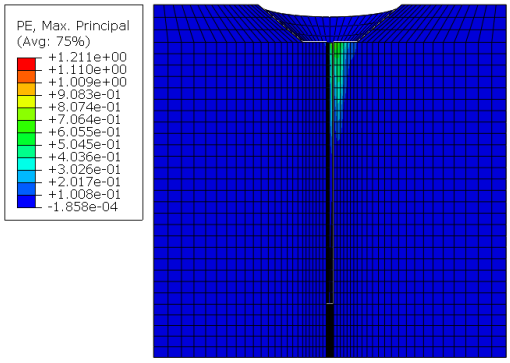	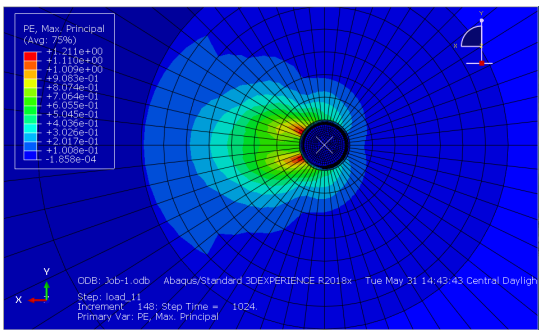
2 m	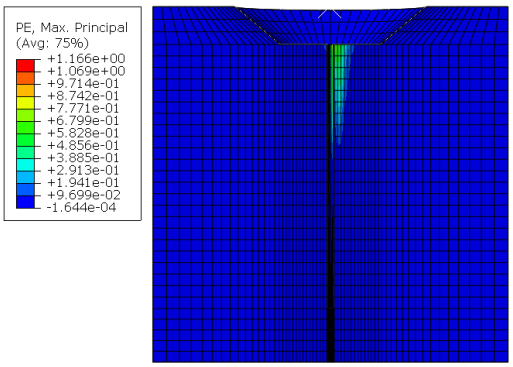	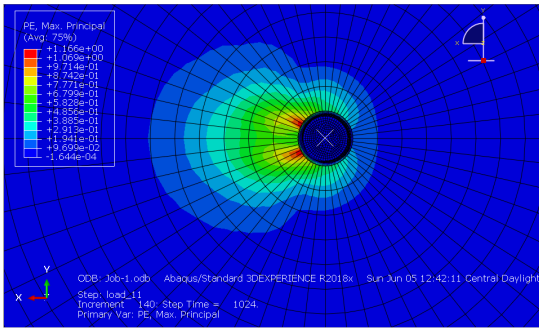

Figure 29. Plastic strain, PE, results depending on scour width, S_w, at pile deflection = 512 mm

4.5.4 Results of Pile deflection depending on Scour Angle, α

In this section, the main parameter of the laterally loaded pile analysis is scour angle, α. There are 6 cases of the scour slope angle: 75 °, 60 °, 40 °, 20 °, 15 °, and 0 °. There are the fixed 5D in scour depth is used. The fixed value of 0.5 m is chosen for the scour width, S_w.

As shown **Figure 30**, the reaction force of the laterally loaded pile is gradually decreased, and the reaction force results at the scour slope angle is equal to between 15 ° and 0 ° show similar results, and this means that the lateral reaction force is converged when the scour slope angle is equal to 15 °. Further, the decreased reaction force is around 3.5 % when the scour slope angle varies from 90 ° to 13 ° and 0 ° (see **Figure 31**).

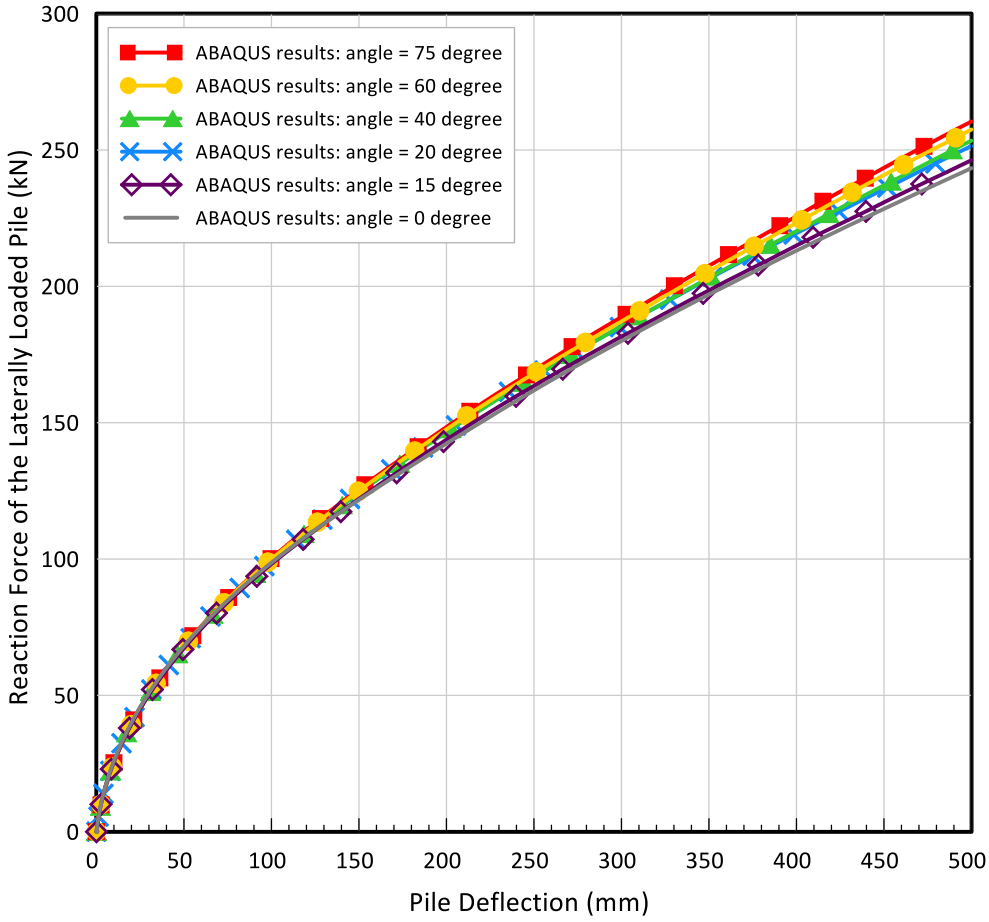

Figure 30. Lateral load vs. Pile deflection curve depending on the scour slope angle, α, with Cam Clay Model

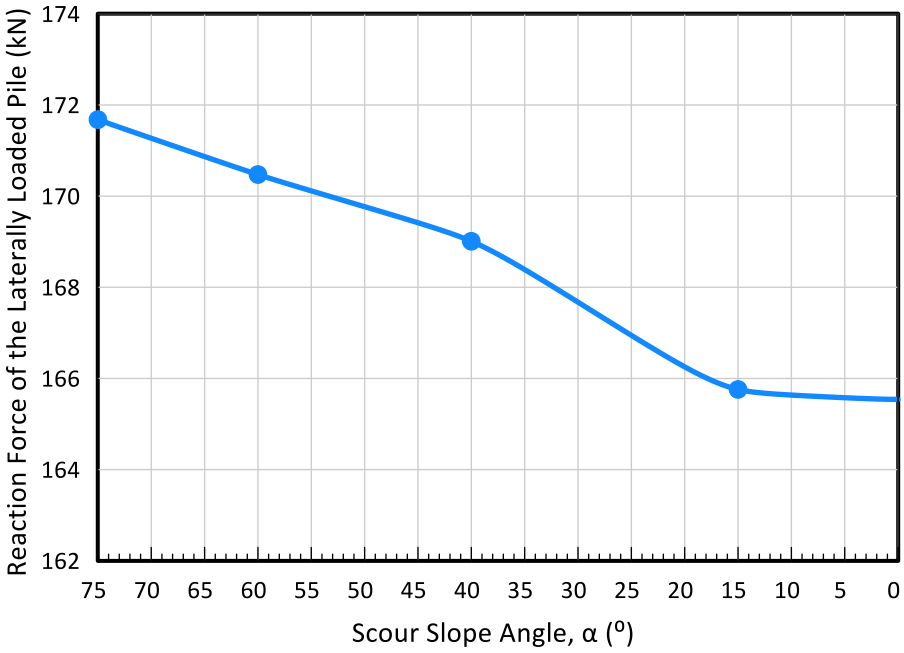

Figure 31. Reaction force distribution depending on scour slope angle, α, at the pile deflection = 0.512 m with Cam Clay Model

Figure 32 is the maximum principal plastic strain (PE) results depending on the scour slope angle at the pile deflection is equal to 512 mm. Mohr-Coulomb model shows plastic strain/deformation at the edge of the scour width geometry. Especially, the larger scour slope angle is applied, the higher PE can be shown. However, as the different manner of Mohr-Coulomb model, the PE in Cam Clay model is expanded smoothly onto the scour slope when the pile is deflected.

α	x-z coordinate	x-y coordinate
75 °	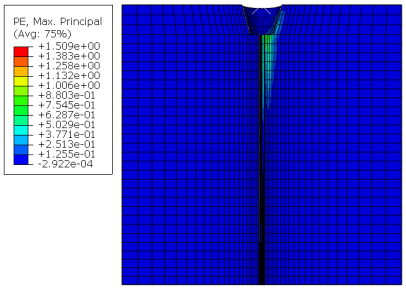	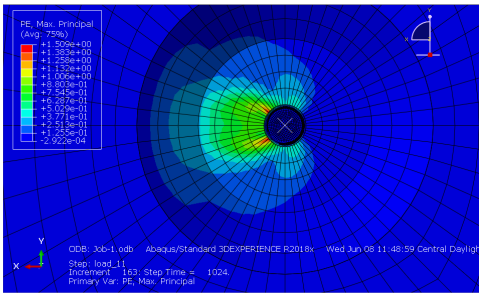
60 °	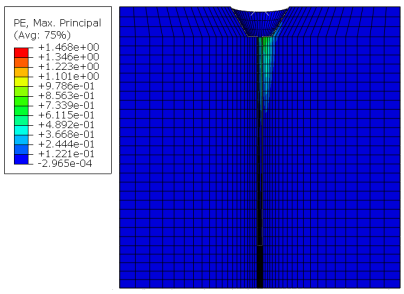	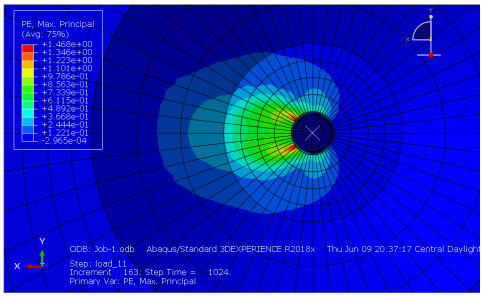
40°	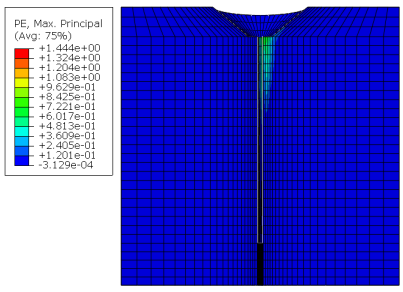	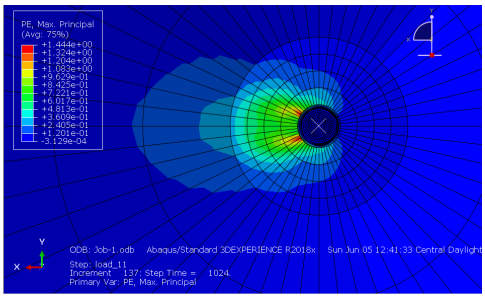
20 °	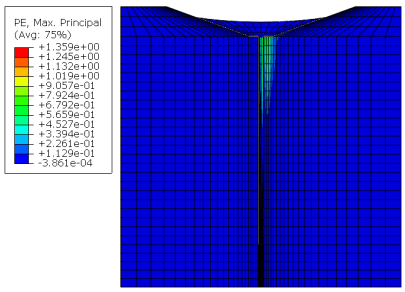	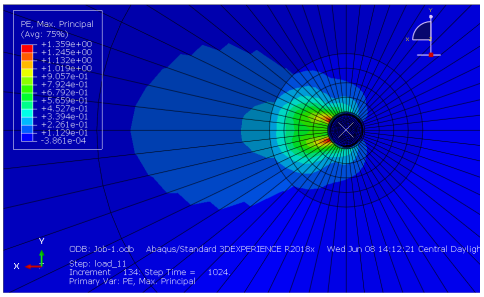
15°	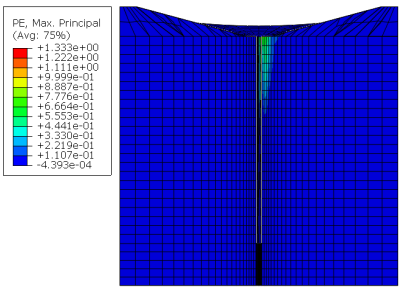	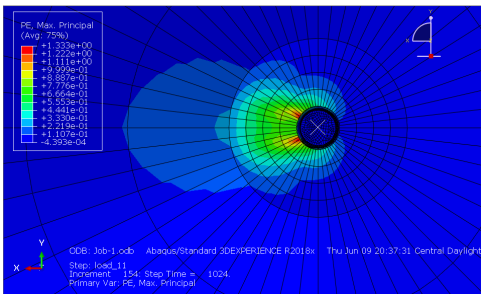

Figure 32. Plastic strain, PE, results depending on scour angle, α, at pile deflection = 512 mm

4.6 Summary

In this chapter, the 3-dimensional laterally loaded pile FE analysis with scour condition is performed based on the material and interface parameters which are calibrated in CHAPTER 3. Two elastoplastic constitutive models are adopted: Mohr-Coulomb model and Cam-Clay model.

Based on the parametric study, both Mohr-Coulomb model and Cam Clay model show that the reaction force of the laterally loaded pile is around 50 % decrease depending on scour depth, S_d. Scour depth, S_w, has an influence on the 10~20 % reaction force decrease, and both Mohr-Coulomb model and Cam Clay model show less than 10 % decrease depending on scour slope angle, α. Based on the numerical results, scour depth, S_d, can be a significant factor to decrease the reaction force of the laterally loaded pile.

Results of the maximum principal plastic strain (PE) are also described in this chapter. Plastic strain/deformation can be shown in both passive and active sides. The main reason of the PE in the passive side is the lateral load. Free-standing soil deformation can induce the PE in the active side. Based on the PE results depending on the scour width, the plastic strain distribution at a specific scour width would be similar to the one when the scour width is infinite, and this means that the reaction force of the laterally loaded pile at the specific scour width is converged in the reaction force at the infinite scour width.

From the PE results depending on the scour slope angle, Mohr-Coulomb model and Cam Clay model show different PE distributions. In the same manner of the scour width cases, the plastic strain distribution at a specific scour slope angle would be similar to the one when the scour width is infinite. Mohr-Coulomb model shows certain plastic strain/deformation at the edge of the scour width geometry. On the other hand, the PE in Cam Clay model is expanded smoothly onto the scour slope.

CHAPTER 5. CONCLUSIONS AND RECOMMENDATIONS

5.1 Conclusions

This thesis focuses on the 3D numerical analysis of the laterally loaded pile using the widely-used commercial software, ABAQUS. Non-scour and scour condition are considered for this thesis. In the scour condition, different cases of scour depth, S_d, scour width, S_w, and scour slope angle, α, are applied for the numerical modeling. From this case study, conclusions can be drawn as follow,

a) In the view of scour depth, S_d, both Mohr-Coulomb model and Cam Clay model show significant the reaction force decrease. In Mohr-Coulomb model, the reaction force of the laterally loaded pile in 6D case is around 50 % decreased compared with the reaction force in non-scour case. Further, Cam clay model also shows that the reaction force of the laterally loaded pile in 8D case is around 50 % decreased compared with the reaction force in non-scour case.

b) For scour width, S_w, 10~20 % reaction force decrease can be shown. Mohr-Coulomb model shows around 20 % decrease comparing 0 m to 4 m, and Cam-Clay model shows around 12 % decrease in comparison 0 m to 2 m.

c) Both Mohr-Coulomb model and Cam Clay model show less than 10 % decrease depending on scour slope angle, α.

d) Based on the parametric study, scour depth, S_d, would be the main factor to have an influence on the changes of the pile capacity.

e) From the plastic strain results depending on the scour width, the plastic strain shape at a specific scour width (2 m both in Mohr-Coulomb model and in Cam clay model)

would be similar to the one when the scour width is infinite, and this means that the reaction force of the laterally loaded pile at the specific scour width is also reached on the reaction force at the infinite scour width.

f) From the PE results depending on the scour slope angle, Mohr-Coulomb model and Cam Clay model show different PE distributions. The PE in Cam Clay model is more smoothly expanded onto the scour slope than Mohr-Coulomb model.

5.2 Recommendations

This thesis discusses the reaction force and plastic strain distribution in scour geometry with respect to scour depth, S_d, scour width, S_w, and scour slope angle, α.. There are several limitations, i.e., scour stability, symmetric scour geometry, etc., Because of these limitations, several recommendations would be proposed to improve this thesis.

a) This thesis describes the reaction force and plastic strain distribution in only the fixed scour geometry which means that scour already exists and this scour is already stable. However, scour effect is one of the time-dependent geometry change problems, so scour geometry, as scour depth, width, and slope angle, can be gradually changed depending on the time. Based on this idea, this thesis can be improved when the time-dependent scour geometry changes are applied for the numerical analysis.

b) As the previous recommendation describes, this study assumes that scour has already existed and this scour is stable. The fact that the scour is stable would mean that the scour process has been already completed, and this is an ultimate case of the scour; however, it is unknown whether the specific scour geometry which is chosen in the

parametric study is the ultimate case or not. Therefore, the future research could be carried out in regard to the ultimate case of the scour geometry based on field and experimental test data.

c) Only symmetric scour geometry is supposed for scour geometry in this thesis. However, in reality, a variety of scour geometry exists. Because of this reason, the numerical analysis for various scour geometry, i.e., asymmetric scour geometry, would be conducted for the future research.

REFERENCES

ABAQUS (2018). ABAQUS User Manual.

AASHTO (2012). AASHTO LRFD Bridge Design Specifications. *American Association of State Highway and Transportation Officials*, Washington, DC, USA.

Achmus, M., Terceros, M., and Thieken, K. (2016). Evaluation of p-y curve approaches for latge diameter monopoles in soft clay. *Proceedings of the Twenty-sixth (2016) International Ocean and Polar Engineering Conference*, Rhodes, Greece, ISOPE-I-16-162.

Ashour, M., Norris, G., and Pilling, P. (1998). Lateral loading of a pile in layered soil using the strain wedge model. *Journal of Geotechnical and Geoenvironmental Engineering*, **124**(4): 303-315.

Briaud, J. L., Ting, F. C. K., Chen, H. C., Gudavalli, R., Perugu, S., and Wei, G. (1999). SRICOS: Prediction of scout rate in cohesive soils at bridge piers. *Journal of Geotechnical and Geoenvironmental Engineering*, **125**(4): 237-246.

Briaud, J. L. (2015). Scour depth at bridge: Method including soil properties. I: Maximum scour depth prediction. *Journal of Geotechnical and Geoenvironmental Engineering*, **141**(2): 04014104.

Bubel, J. and Grabe, J. (2012). Stability of submarine foundation pits. *Offshore Site Investigation and Geotechnics: Integrated Technologies - Present and Future*, London, UK, SUT-OSIG-12-37.

Bubel, J, and Grabe, J. (2012). Stability of submarine foundation pits under wave loads. *Proceedings of the ASME 2012 31st International Conference on Ocean, Offshore and Arctic Engineering*. **4**: 11-19.

Chavan, V. S., Chen, S., Shanmugam, N. S., Tang, W., Diemer, J., Allan, C., Braxtan, N., Shukla, T., Chen, T., and Slocum, Z. (2022). An analysis of local and combined (global) scours on piers-on-bank bridges. *CivilEng*, **3**(1): 1-20.

Chen, L. and Poulos, H. G. (1993). Analysis of pile-soil interaction under lateral loading using infinite and finite elements. *Computers and Geotechnics*, **15**: 189-220.

Coduto, D. P. (2001). Foundation Design: Principles and Practices (2nd ed.). New Jersey, NJ: Prentice Hall.

Dao TPT. (2011). Validation of PLAXIS embedded piles for lateral loading. Master's thesis. Delft University of Technology.

Guo, X., Liu, J., Yi, P., Feng, X., Han, C. (2022). Effect of local scour on failure envelops of offshore monopiles and caissons. *Applied Ocean Research*, **118**: 103007.

He, B., L, Y., Wang, L, Hong, Y., and Zhu, R. (2019). Scour effects on the lateral behavior of a large-diameter monopile in soft clay: Role of stress history. *Journal of Marin Science and Engineering*, **7**: 170.

Jia, J. (2018). Soil dynamics and Foundation Modeling: Offshore and Earthquake Engineering. Springer.

Jia, N., Liu, J., and Wang, X. (2022). Numerical investigation into lateral behavior of monopile due to scour enhanced: Role of state-dependent dilatancy. *Applied Sciences*, **12**(2): 921.

Kim, Y. and Jeong, S. (2011). Analysis of soil resistance on laterally loaded piles based on 3D soil-pile interaction. *Computers and Geotechnics*, **38**: 248-257.

Lee, J. and Lee, Y. (2014). Investigation of pile behaviour according to interface properties-comparison between pile model test using close range photogrammetry and numerical analysis. *Journal of Korean Geotechnical Society*, **30**(9): 29–39.

Li, F., Han, J, and Lin, C. (2013). Effects of scour on the behavior of laterally loaded single piles in Marine clay. *Marine Georesources & Geotechnology*. **31**: 271-289.

Liang, F., Zhang, H., and Chen, S. (2018). Effect of vertical load on the lateral response of offshore piles considering scour-hole geometry and stress history in marine clay. *Ocean Engineering*, **158**: 64-77.

Lin, C., Han, J., Bennett, C., and Parsons, R. L. (2014). Behavior of laterally loaded piles under scout conditions considering the stress history of undrained soft clay. *Journal of Geomechnical and Geoenvironmental Engineering*, **140**(6): 06014005.

Lin, C., Han, J., Bennett, C., and Parsons, R. L. (2016). Analysis of laterally loaded piles in soft clay considering scour-hole dimension. *Ocean Engineering*, **111**: 461-470.

Lin, Y. and Lin, C. (2019). Effects of scour-hole dimensions on lateral behavior of piles in sands. *Computers and Geotechnics*, **111**: 30-41.

Lin, Y. and Lin, C. (2020). Scour effects on lateral behavior of pile groups in sands. *Ocean Engineering*, **208**: 107420.

Mardfekri, M., Gardoni, P., and Roesset, J. M. (2013). Modeling laterally loaded single piles accounting for nonlinear soil-pile interactions. *Journal of Engineering*, 2013: 243179.

Potts, D.M. and Zdravković, L. (1999). Finite element analysis on geotechnical engineering – Theory. Thomas Telford Publishing, Thomas Telford Ltd, 1 Heron Quay, London, 68-72

Potts, D.M. and Zdravković, L. (2001). Finite element analysis on geotechnical engineering – Application. Thomas Telford Publishing, Thomas Telford Ltd, 1 Heron Quay, London, 280-289

Richardson, E.V., and Davis, S.R. (2001). Evaluating scour at bridges. 4th ed. Washington, DC: Federal Highway Administration; FHWA NHI 01–001 (HEC 18).

Wang, Z., Hu, R., Leng, H., Liu, H., Bai, Y., and Lu, W. (2020). Deformation analysis of large diameter monopiles of offshore wind turbines under scour. *Applied Sciences*, **10**(21): 7579.

Wood, D. M. (1990). Soil behaviour and critical state soil mechanics. Cambridge University Press, The Edinburgh Building, Cambridge CB2 8RU, UK.

Yang, J. and Mu, F. (2008). Use of state-dependent strength in estimating end bearing capacity of piles in sand. *Journal of Geotechnical and Geoenvironmental Engineering*, **134**(7): 1010-1014

Yang, Z. and Jeremic, B. (2002). Numerical analysis of pile behaviour under lateral loads in layered elastic-plastic soils. *International Journal for Numerical and Analytical Methods in Geomechanics*, **26**: 1385-1406.

Zania, V. and Hededal, O. (2012). Friction effects on lateral loading behavior of rigid piles. GeoCongress 2012, Oakland, California, USA, 366-375.

Zhang, H., Chen, S., and Liang, F. (2017). Effects of scour-hole dimensions and soil stress history on the behavior of laterally loaded piles in soft clay under scour conditions. *Computers and Geotechnics*, **84**: 198-209.

Zhang, F., Dai, G., and Gong, W. (2021). Analytical method for laterally loaded piles in soft clay considering the influence of soil outside the scour hole on the effective overburden pressure. *Acta Geotechnica*, **16**: 2963–2974.

VITA

Jungmin Lee was born in Seoul, Republic of Korea (South Korea). She earned her Bachelor's degree in 2011 and Master in Engineering in 2013 at Seoul National University of Science and Technology. She will be graduate from Louisiana State University in Summer 2022. After her graduation, she will join the new research group to another university for her next research journey.